



# 1 **Insights into seasonal variation of wet deposition over Southeast Asia** 2 **via precipitation adjustment from the findings of MICS-Asia III**

3 Syuichi Itahashi<sup>1,2</sup>, Baozhu Ge<sup>3,4,5</sup>, Keiichi Sato<sup>6</sup>, Zhe Wang<sup>3,5,7</sup>, Junichi Kurokawa<sup>6</sup>, Jiani Tan<sup>8,9</sup>, Kan  
4 Huang<sup>9,10</sup>, Joshua S. Fu<sup>9</sup>, Xuemei Wang<sup>11</sup>, Kazuyo Yamaji<sup>12</sup>, Tatsuya Nagashima<sup>13,14</sup>, Jie Li<sup>3,4,5</sup>, Mizuo  
5 Kajino<sup>2,14</sup>, Gregory R. Carmichael<sup>15</sup>, Zifa Wang<sup>3,4,5</sup>

6 <sup>1</sup>Environmental Science Research Laboratory, Central Research Institute of Electric Power Industry (CRIEPI), Abiko, Chiba  
7 270–1194, Japan

8 <sup>2</sup>Meteorological Research Institute (MRI), Tsukuba, Ibaraki 305–0052, Japan

9 <sup>3</sup>State Key Laboratory of Atmospheric Boundary Layer Physics and Atmospheric Chemistry (LAPC), Institute of  
10 Atmospheric Physics (IAP), Chinese Academy of Sciences (CAS), Beijing 100029, China

11 <sup>4</sup>Collage of Earth Science, University of Chinese Academy of Sciences, Beijing 100049, China

12 <sup>5</sup>Center for Excellence in Urban Atmospheric Environment, Institute of Urban Environment, Chinese Academy of Sciences  
13 (CAS), Xiamen 361021, China

14 <sup>6</sup>Asia Center for Air Pollution Research (ACAP), 1182 Sowa, Nishi-ku, Niigata, Niigata 950–2144, Japan

15 <sup>7</sup>Research Institute for Applied Mechanics (RIAM), Kyushu University, Fukuoka 816-8580, Japan

16 <sup>8</sup>Multiphase Chemistry Department, Max Planck Institute for Chemistry, Mainz 55128, Germany

17 <sup>9</sup>Department of Civil and Environmental Engineering, University of Tennessee, Knoxville, TN 37996, USA

18 <sup>10</sup>Department of Environmental Science and Engineering, Fudan University, Shanghai 200433, China

19 <sup>11</sup>Institute for Environment and Climate Research, Jinan University, Guangzhou 510275, China

20 <sup>12</sup>Graduate School of Maritime Sciences, Kobe University, Kobe, Hyogo 658–0022, Japan

21 <sup>13</sup>National Institute for Environmental Studies (NIES), Tsukuba, Ibaraki 305–8506, Japan

22 <sup>14</sup>Faculty of Life and Environmental Sciences, University of Tsukuba, Tsukuba, Ibaraki 305–8572, Japan

23 <sup>15</sup>Center for Global and Regional Environmental Research, University of Iowa, Iowa City, IA 52242, USA

24 *Correspondence to:* Syuichi Itahashi (isyuichi@criepi.denken.or.jp)

25

26 **Abstract.** Asia has attracted research attention because it has the highest anthropogenic emissions in the world, and the  
27 Model Inter-Comparison Study for Asia (MICS-Asia) Phase III was carried out to foster our understanding on the status of  
28 air quality over Asia. This study analyzed wet deposition in Southeast Asian countries (Myanmar, Thailand, Lao People's  
29 Democratic Republic (PDR), Cambodia, Vietnam, the Philippines, Malaysia, and Indonesia) with the aim of providing  
30 insights into the seasonal variation of wet deposition. Southeast Asia was not fully considered in MICS-Asia Phase II due to  
31 a lack of observational data; however, the analysis period of MICS-Asia III, namely, the year 2010, is covered by ground  
32 observations of the Acid Deposition Monitoring Network in East Asia (EANET), and the coordinated simulation domain  
33 was extended to cover these observation sites. The analyzed species are wet depositions of S (sulfate aerosol, sulfur dioxide  
34 (SO<sub>2</sub>), and sulfuric acid (H<sub>2</sub>SO<sub>4</sub>)), N (nitrate aerosol, nitrogen monoxide (NO), nitrogen dioxide (NO<sub>2</sub>), and nitric acid  
35 (HNO<sub>3</sub>)), and A (ammonium aerosol and ammonia (NH<sub>3</sub>)). The wet deposition simulated with seven models driven by



36 unified meteorological model in MICS-Asia III was used with the ensemble approach, which effectively modulates the  
37 differences in performance among models. By comparison with EANET observations, although the seven models generally  
38 captured the wet depositions of S, N, and A, there were difficulties capturing these in some cases. This failure of models is  
39 considered to be related to the difficulty in capturing the precipitation in Southeast Asia, especially during the dry and wet  
40 seasons. To overcome this, a precipitation-adjusted approach which scaling the modeled precipitation to the observed value  
41 was applied, and it was demonstrated that the model performance was improved. Satellite measurements were also used to  
42 adjust for precipitation data, which worked well to account for spatio-and-temporal precipitation patterns, especially in the  
43 dry season. As the statistical scores were mostly improved by this adjustment, the estimation of wet deposition with  
44 precipitation adjustment was considered to be superior. To utilize satellite measurements, the spatial distribution of wet  
45 deposition was revised. Based on this revision, it was found that Vietnam, Malaysia, and Indonesia were upward-corrected  
46 and Myanmar, Thailand, Lao PDR, Cambodia, and the Philippines were downward-corrected; these corrections were up to  
47  $\pm 40\%$ . The improved accuracy of precipitation amount was key to estimating wet deposition in this study. These results  
48 suggest that the precipitation-adjusted approach has the potential to obtain accurate estimates of wet deposition through the  
49 fusion of models and observations.

50

## 51 **1 Introduction**

52 With the recent acceleration of its emission from anthropogenic sources, Asia has the world's highest acid deposition (Vet et  
53 al., 2014). To measure atmospheric concentrations and depositions in Asia, the Acid Deposition Monitoring Network in East  
54 Asia (EANET) has maintained a Asian observation network since 2000. At present, 13 countries participate in EANET  
55 (EANET, 2020a). This observational study is essential for understanding the status of air quality over Asian countries.  
56 Another approach is analysis based on chemical transport models (CTMs), which numerically simulate various processes of  
57 air pollutants such as emission, transport, chemical reactions, and deposition. CTMs are based on the forefront scientific  
58 algorithms; however, uncertainties in each process are critical (Carmichael et al., 2008a). Therefore, relying on single CTM  
59 can lead to the misinterpretation of phenomena. In order to account for uncertainties in CTMs, multi-model inter-comparison  
60 study is vital. The Model Inter-Comparison Study for Asia (MICS-Asia) has been conducted over Asian countries: Phase I  
61 during 1998–2000 (Carmichael et al., 2002), Phase II during 2003–2008 (Carmichael et al., 2008b), and Phase III during  
62 2010–2020. Phase III contains three parts: Topic 1, involving the study of comparison and evaluation of current air quality  
63 models (Akimoto et al., 2019, 2020; Chen et al., 2019; Itahashi et al., 2020; Kong et al., 2020; Li et al., 2019); Topic 2,  
64 involving the development of emission inventories for Asia (Li et al., 2017); and Topic 3, involving the study of interactions  
65 between air quality and climate change (Gao et al., 2018, 2020). In terms of deposition, Itahashi et al. (2020) presented an  
66 overview of model performances in MICS-Asia III and reported that models generally captured the observed wet deposition;  
67 however, it was clarified that models underestimated the wet deposition of sulfate aerosol ( $\text{SO}_4^{2-}$ ), and the differences in



68 modeling performance were largest for nitrate aerosol ( $\text{NO}_3^-$ ). For sulfur species, Tan et al. (2020) analyzed the oxidation  
69 ratio of sulfur (i.e., the conversion ratio from sulfur dioxide ( $\text{SO}_2$ ) to  $\text{SO}_4^{2-}$ ) and found that models underestimated the  
70 oxidation rate and thus underestimated the concentration and deposition of  $\text{SO}_4^{2-}$ . In China, which is one of the dominant  
71 anthropogenic emission sources in Asia, publicly available observational data were once quite limited (Chan and Yao, 2008).  
72 However, a nationwide estimation of nitrogen burden has been reported by Liu et al. (2013) and a national observation  
73 network has been established (see Ge et al., 2020, and references therein). The use of large amounts of observational data for  
74 China is one of the advantages of MICS-Asia III. Ge et al. (2020) analyzed the reactive nitrogen deposition over China, and  
75 the results indicated that wet deposition of ammonium aerosol ( $\text{NH}_4^+$ ) was underestimated by all models across China.  
76 This study focuses on Southeast Asia. This area has received research attention due to its severe air pollution, which in some  
77 cases is caused by emissions from biomass burning (Itahashi et al., 2018; Vadrevu and Justice, 2011). Recently, the 7-  
78 Southeast Asian Studies (7SEAS) program was formed to facilitate interdisciplinary research (Lin et al. 2013; Reid et al.  
79 2013). Due to the lack of observational data from EANET, the status of deposition over Southeast Asia was not fully  
80 analyzed in Phase II of MICS-Asia. However, in Phase III, EANET observational data are available and Southeast Asian  
81 countries are fully covered by the simulation domain in CTMs. A total of eight Southeast Asian countries participate in  
82 EANET. Fig. 1 shows a map of the EANET observation sites over Southeast Asia whose data were used in this study.  
83 Hereafter, Myanmar, Thailand, the Lao People's Democratic Republic (PDR), Cambodia, and Vietnam are taken to  
84 constitute continental Southeast Asia, and the Philippines, Malaysia, and Indonesia are taken to constitute oceanic Southeast  
85 Asia. This paper is organized as follows. Section 2 describes the MICS-Asia Phase III in terms of the framework of model  
86 intercomparison and observational data. Section 3 presents the results of the analysis of the wet depositions over Southeast  
87 Asia and discusses the problems in the current models. Section 4 explains how the precipitation-adjusted approach was  
88 applied and demonstrates that it improved the modeling performance for wet deposition. The precipitation data used to  
89 linearly scale the modeled precipitation were EANET observational data reported previously (Itahashi et al., 2020), and  
90 satellite measurements were also used in this study to advance this previous study. Furthermore, the wet deposition amount  
91 and the fraction of wet deposition occurring during the dry and wet seasons are presented before and after the application of  
92 the precipitation-adjusted approaches. Additionally, revised wet deposition maps over Southeast Asia are presented. Finally,  
93 Section 5 dedicates to the summary of this study and looks toward the next Phase IV of MICS-Asia.

94

## 95 **2 Framework of MICS-Asia Phase III for wet deposition**

### 96 **2.1 Model description**

97 In MICS-Asia Phase III, the targeted year was 2010. The participating model was requested to submit the monthly  
98 accumulated dry and wet deposition amounts of S species ( $\text{SO}_4^{2-}$ ,  $\text{SO}_2$ , sulfuric acid ( $\text{H}_2\text{SO}_4$ )), N species ( $\text{NO}_3^-$ , nitrogen  
99 monoxide (NO), nitrogen dioxide ( $\text{NO}_2$ ), nitric acid ( $\text{HNO}_3$ )), and A species ( $\text{NH}_4^+$  and ammonia ( $\text{NH}_3$ )). In total, nine



00 models (M1, M2, M4, M5, M6, M11, M12, M13, and M14; these numbers are unified for MICS-Asia Phase III) were used  
01 in this deposition analysis; these models are summarized in an overview paper (Itahashi et al., 2020, Table 1). In this study,  
02 seven models (M1, M2, M4, M5, M6, M11, and M12) that using the same meteorological fields simulated by the Weather  
03 Research and Forecasting (WRF) model version 3.4.1 (Skamarock et al., 2008) were selected. Models M1, M2, M4, M5, and  
04 M6 were from the Community Multiscale Air Quality (CMAQ) modeling system (Byun and Schere, 2006) developed by the  
05 U.S. Environmental Protection Agency (EPA), but were configured differently in terms of model version, horizontal and  
06 vertical advection/diffusion schemes, gas-phase and aerosol chemistry, dry and wet deposition schemes, and lateral boundary  
07 conditions. M11 was the nested air quality prediction model system (NAQPMS) developed by the Institute of Atmospheric  
08 Physics (IAP), Chinese Academy of Sciences (CAS) (Ge et al., 2014; Li et al., 2016), and M12 was the non-hydrostatic  
09 mesoscale model coupled with chemistry transport model (NHM-Chem) developed by the Meteorological Research Institute  
10 (MRI), Japan (Kajino et al., 2019a). The input emissions data were unified for all models using the MIX inventory (Li et al.,  
11 2017). The details of the configurations and the verification of model performances have been published for gas (Kong et al.,  
12 2020; Li et al., 2019), aerosols (Chen et al., 2019), and deposition (Ge et al., 2020; Itahashi et al., 2020; Tan et al., 2020).

13 To reduce the uncertainty in various processes and configurations of the models, an ensemble approach was applied to the  
14 model results. In the findings of MICS-Asia Phase II, it was clarified that the ensemble means, rather than means of  
15 individual models, agreed well with observed sulfate and total ammonium levels (Hayami et al., 2008). In other model  
16 comparisons study, the Air Quality Model Evaluation International Initiative (AQMEII), which focuses on North America  
17 and Europe, model performance was improved by using the ensemble mean (Solazzo et al., 2012). In MICS-Asia Phase III,  
18 an ensemble approach for the gas species NO<sub>2</sub>, NH<sub>3</sub>, and CO (Kong et al., 2020), O<sub>3</sub> (Li et al., 2019), aerosols (Chen et al.,  
19 2019), and depositions (Ge et al., 2020; Itahashi et al., 2020; Tan et al., 2020) has been used and has generally performed  
20 well compared with each model. The equation used to calculate the ensemble mean (ENS) is as follows:

$$21 \quad ENS = \frac{1}{N} \sum WD \quad (1)$$

22 where WD is the wet deposition, and N is the number of models, which is 7 in this study. The simple ensemble based on the  
23 arithmetic average was applied in this study. The calculated ENS was compared with observations over Southeast Asia.

## 25 **2.2 EANET observations**

26 In EANET, wet deposition is observed by a wet-only sampler that is designed to collect samples during precipitation  
27 (EANET, 2010). The locations of the observation sites used in this study are plotted in Fig. 1, and Table 1 shows the latitude,  
28 longitude, altitude, and classification information for each. The identification numbers of the sites are unified with the  
29 overview paper of deposition analysis of MICS-Asia III (Itahashi et al., 2020). The sites classification are defined as follows:  
30 urban sites are located urbanized and industrialized areas; rural sites are located more than 20 km away from large pollution



31 sources; and remote sites are located more than 50 km away from large pollution sources and more than 500 m away from  
32 main roads. Ion chromatography was used to analyze anions ( $\text{SO}_4^{2-}$  and  $\text{NO}_3^-$ ) and cations ( $\text{NH}_4^+$ ). The observational data  
33 were checked by ion balance and conductivity agreement. From the duration of precipitation coverage and total precipitation  
34 amount, the data completeness was determined (EANET, 2000). The sampling intervals differed from site to site; daily,  
35 weekly, or 10 days (EANET, 2020b). The monthly accumulated wet deposition at each site were used for the model  
36 evaluation. Over the analyzed period, the observation data at Vientiane (No. 37; Table 1) in Lao PDR was not available, and  
37 not analyzed in this study.

38 To evaluate the model performance compared with EANET observations, the three statistical metrics of correlation  
39 coefficient (R), normalized mean bias (NMB), and normalized mean error (NME) were used. These are defined as follows:

$$40 \quad R = \frac{\sum_1^N (O_i - \underline{O})(M_i - \underline{M})}{\sqrt{\sum_1^N (O_i - \underline{O})^2} \sqrt{\sum_1^N (M_i - \underline{M})^2}} \quad (2)$$

$$41 \quad NMB = \frac{\sum_1^N (M_i - O_i)}{\sum_1^N O_i} \quad (3)$$

$$42 \quad NME = \frac{\sum_1^N |M_i - O_i|}{\sum_1^N O_i} \quad (4)$$

43 where N is the total number of paired observations (O) and models (M). Additionally, the percentages within a factor of 2  
44 (FAC2), within a factor of 3 (FAC3), and within a factor of 5 (FAC5) were also calculated to judge the agreement between  
45 observations and models

46

## 47 **3 Results**

### 48 **3.1 Seasonal variation of wet deposition for each country over Southeast Asia**

#### 49 **3.1.1 Myanmar**

50 Myanmar has one EANET site for wet deposition, at Yangon (No. 30; Table 1). A comparison between observational and  
51 model-simulated data for precipitation and wet depositions are shown in Fig. 2. In 2010, the observed monthly accumulated  
52 precipitation was zero from January to April, 7.5 mm in November, 25.4 mm in December, and around 300 mm from May to  
53 October. Hereafter, precipitation of 50 mm/month is used as the index to divide the dry and wet seasons. Based on this  
54 criterion, the dry and wet seasons were clearly characterized from observed precipitation; however, the model simulated light  
55 precipitation of around 20 mm even during the dry season, and underestimated precipitation during the wet season. Due to  
56 the seasonal variation in the observed precipitation, the observed wet deposition of S, N, and A also exhibited a clear  
57 seasonal dependency during the dry and wet seasons. Compared with the observed wet deposition, the model generally  
58 overestimated the wet deposition during the dry season and underestimated it during the wet season. These results indicate



59 that the model performance for precipitation could be a critical factor in determining the model performance for wet  
60 deposition. The statistical performance of the simulated wet deposition of S, N, and A is listed in Table 2. The ENS results  
61 showed a good correlation with the observed data, with an R of around 0.8; however, there was a large underestimation for  
62 wet deposition, with an NMB greater than  $-70\%$  and an NME greater than  $80\%$ . As suggested by the observed monthly wet  
63 deposition amount shown in Fig. 2, these underestimations were mainly due to the model performance during the wet  
64 season.

65

### 66 3.1.2 Thailand

67 In Thailand, there are six EANET sites for wet deposition, namely, Bangkok (No. 31), Samutprakarn (No. 32), Pathumthani  
68 (No. 33), Khanchanaburi (No. 34), Nakhon Ratchasima (No. 35), and Chiang Mai (No. 36; Table 1). A comparison between  
69 the observed and simulated precipitation and wet deposition is shown in Fig. 3. The dry and wet seasons were clearly  
70 distinct; the wet season is from May to October at Bangkok (No. 31), Samutprakarn (No. 32), Pathumthani (No. 33),  
71 Khanchanaburi (No. 34), and Chiang Mai (No. 36), and from March to October at Nakhon Ratchasima (No. 35). The model  
72 generally overestimated precipitation during the dry season at all six sites. For the wet deposition of S and N, the model  
73 tended to underestimate at Bangkok (No. 31), Samutprakarn (No. 32), Pathumthani (No. 33), and Nakhon Ratchasima (No.  
74 35) during the wet season, which is related to the underestimation of precipitation itself, whereas the model overestimated  
75 precipitation at Khanchanaburi (No. 34) and Chiang Mai (No. 36) throughout the year. The results of the statistical analyses  
76 are listed in Table 3. ENS showed underestimation for the wet deposition of S, N, and A, with an NMB of  $-20$  to  $-50\%$  and  
77 an NME larger than  $80\%$ . Additionally, the correlation between the observed and simulated data was small, especially for S,  
78 which showed no linear correlation. The observed wet deposition amount was higher in the wet season, but the amount  
79 calculated throughout the year was nearly constant.

80

### 81 3.1.3 Cambodia

82 Cambodia has one EANET site for wet deposition, at Phnom Penh (No. 38; Table 1). A comparison between the observed  
83 and simulated precipitation and wet deposition is shown in Fig. 4. The wet season (monthly accumulated precipitation more  
84 than  $50$  mm) lasted from March to November. According to this precipitation pattern, higher wet depositions of S, N, and A  
85 were also observed during the wet season. However, the ENS underestimated the wet deposition amount during the wet  
86 season, especially in June and July; this is related to the underestimation of precipitation in these months. The statistical  
87 analysis is summarized in Table 4. The correlation between the observed and simulated data was low, especially for the wet  
88 deposition of S, while the NMB and NME were around  $-70\%$  and  $70$ – $80\%$ , respectively, for the wet depositions of S, N, and  
89 A. That is, there were some difficulties in capturing the wet deposition at this site, even using the ENS.

90



### 91 3.1.4 Vietnam

92 Vietnam has four EANET sites for wet deposition, namely, Da Nang (No. 39), Hanoi (No. 40), Hoa Binh (No. 41), and Cuc  
93 Phuong (No. 42; Table 1). A comparison between the observed and simulated precipitation and wet deposition is shown in  
94 Fig. 5. Compared with other countries in continental Southeast Asia, precipitation patterns during the dry and wet seasons  
95 were relatively well captured at the four sites in Vietnam. Accordingly, the wet depositions of S, N, and A obtained by the  
96 ENS can generally reproduce the observed data to an acceptable level. The results of the statistical analysis are shown in  
97 Table 5. As can be seen from the table, as well as from Fig. 5, the statistical scores for Vietnam were better than those for the  
98 other countries in continental Southeast Asia. The R value was around 0.5–0.6, while the NMB was around –35% for the wet  
99 deposition of S and N and around +15% for the wet deposition of A. The NME was around +50%, which was smaller than  
00 for other countries in continental Southeast Asia.

01

### 02 3.1.5 Philippines

03 There are three EANET sites for wet deposition in the Philippines, namely, Metro Manila (No. 43), Los Baños (No. 44), and  
04 Mt. Sto. Tomas (No. 45; Table 1). A comparison between the observed and simulated precipitation and wet deposition is  
05 shown in Fig. 6. The wet season was classified from June to December at Metro Manila (No. 43) and Los Baños (No. 44),  
06 and from April to November at Mt. Sto. Tomas (No. 45). Generally, the model captured the seasonal variation of  
07 precipitation adequately, but the precipitation was overestimated during the dry season. The statistical analysis is presented  
08 in Table 6. For the wet deposition of S, R was 0.79 and NMB and NME were +11.4% and +58.0%, respectively. The ENS  
09 captured the wet deposition of S adequately. However, the NME values were worse for the wet deposition of N and A. For  
10 example, the NME for the wet deposition of A was greater than +100%. In particular, as shown in Fig. 6, the models could  
11 not reproduce the peaks of the wet deposition of N and A in October at either Metro Manila (No. 43) or Los Baños (No. 44).  
12 Additionally, the wet deposition of N and A was also underestimated for other months during the wet season at the same two  
13 sites. This phenomenon should be further studied in the future to improve the simulation of wet deposition at these sites.

14

### 15 3.1.6 Malaysia

16 There are four EANET sites for wet deposition in Malaysia, namely, Petaling Jaya (No. 46), Tanah Rata (No. 47), Kuching  
17 (No. 48), and Danum Valley (No. 49; Table 1). A comparison between the observed and simulated precipitation and wet  
18 deposition is shown in Fig. 7. Compared with other countries, the four sites in Malaysia did not show clear dry and wet  
19 seasons, and precipitation amounts were consistently large over the course of the year. Therefore, the division into dry and  
20 wet seasons was not conducted for the four sites in Malaysia. At Danum Valley (No. 49), the observed precipitation was  
21 greater than 50 mm in all months except February. However, there was a lack of wet deposition observations at Danum



22 Valley (No. 49). As shown in Fig. 7, the models had difficulties capturing the behavior of wet deposition over Malaysia. At  
23 Petaling Jaya (No. 46) and Kuching (No. 48), the ENS underestimated the wet deposition of S and N and overestimated the  
24 wet deposition of A. At Tanah Rata (No. 47), wet deposition was dramatically overestimated for all species. The results of  
25 the statistical analysis are listed in Table 7. There was a moderate correlation between the observations and simulations for  
26 the wet deposition of S and N, and the NMB and NME were highest for the wet deposition of S. It should be noted that the  
27 wet deposition of A showed much higher NMB and NME values and a lower value of R; this is due to the fact that the wet  
28 deposition of A was overestimated at all four sites in Malaysia (Fig. 7).

29

### 30 **3.1.7 Indonesia**

31 Indonesia has five EANET sites for wet deposition, namely, Jakarta (No. 51), Bandung (No. 52), Serpong (No. 53),  
32 Kototabang (No. 50), and Maros (No. 54; Table 1). A comparison between the observed and simulated precipitation and wet  
33 deposition is shown in Fig. 8. Compared with other countries in continental Southeast Asia, the dry season was shorter in  
34 Indonesia, occurring only in April in Jakarta (No. 51), Bandung (No. 52), and Serpong (No. 53), which are located on Java  
35 Island; in August in Kototabang (No. 50), which is located on Sumatra Island; and in January and February in Maros (No.  
36 54), which is located on Sulawesi Island. The observed wet deposition of S, N, and A in these limited dry seasons was  
37 generally lower than during the wet season; however, no difference in the simulated wet deposition of S, N, and A was  
38 observed between the wet and dry season. The reason for this failure was that the model did not show the reduced  
39 precipitation amounts seen in observations during these dry seasons. The results of the statistical analysis are listed in Table  
40 8. A moderate correlation between observations and simulations was found for the wet deposition of S, N, and A, but the  
41 ENS overestimated the wet deposition of S, N, and A, especially for S, with an NMB of +65.6% and an NME larger than  
42 100%.

43

## 44 **4 Discussion**

### 45 **4.1 Proposal of precipitation-adjusted approach over Southeast Asia**

46 As presented in Sect. 3, although the model performances in MICS-Asia III based on an ensemble approach generally  
47 captured the observed wet deposition over Southeast Asia, there were some difficulties in capturing the observed values.  
48 This difficulty stemmed from the inaccuracy of the modeled precipitation, which is fundamentally important for simulating  
49 the wet deposition. In the overview paper of MICS-Asia III, ways to improve the model performances were considered and  
50 the precipitation-adjusted approach was selected (Itahashi et al., 2020). The precipitation-adjusted approach linearly scales  
51 the precipitation to obtain the precipitation-adjusted wet deposition via the following equation:



$$52 \quad \text{Adjusted } WD = \sum_{\text{monthly}} \text{Original } WD_{\text{model}} \times \frac{\sum_{\text{monthly}} P_{\text{observation}}}{\sum_{\text{monthly}} P_{\text{model}}} \quad (5)$$

53 where  $WD_{\text{model}}$  is the original wet deposition by model, and  $P_{\text{model}}$  and  $P_{\text{observation}}$  are the modeled and observed precipitation,  
54 respectively. Here, supposing that the errors in the modeled precipitation are linearly associated to the errors in the modeled  
55 wet deposition. This approach has been used in previous studies in the U.S.A. (Appel et al., 2011; Zhang et al., 2018) and  
56 East Asia (Itahashi, 2018; Saya et al., 2018). Following our previous work in MICS-Asia III for deposition (Itahashi et al.,  
57 2020), wet depositions were adjusted on a monthly time scale and then the annual wet deposition was recalculated from  
58 precipitation-adjusted monthly wet deposition. Adjustment of shorter time scales is difficult because the modeled  
59 precipitation ( $P_{\text{model}}$  in Eq. (5)) approaches zero, which leads to unreasonably large values, and vice versa for larger time  
60 scales. The precipitation-adjusted approach using EANET observational data is hereafter called AO (adjusted by observation  
61 at EANET site).

62 The precipitation-adjusted approach was shown to be effective for improving the modeling reproducibility in MICS-Asia III  
63 (Itahashi et al., 2020). However, this approach has a limitation in that the adjusted wet deposition was obtained only at  
64 locations corresponding to EANET observation sites, and hence the adjusted wet deposition was spatially limited. To  
65 overcome this limitation, in this study, we additionally used a satellite dataset; this precipitation-adjusted approach is  
66 hereafter called AS (adjusted by satellite measurement). For this purpose, the Tropical Rainfall Measuring Mission (TRMM)  
67 multi-satellite precipitation analysis (TMPA) dataset was applied (Huffman et al., 2007). The used product is the latest  
68 version 7 of the 3B43 dataset, which provides monthly precipitation with the most accurate precipitation estimate covering  
69  $50^{\circ}$  S to  $50^{\circ}$  N (TRMM, 2011). The gridded data of  $0.25 \times 0.25^{\circ}$  were converted into the simulation domain used in MICS-  
70 Asia Phase III. For the AO and AS approaches, wet deposition in each of the seven models was first adjusted on a monthly  
71 time scale, and then the ENS was calculated using Eq. (1).

72 A comparison among the WRF simulation, EANET surface observations, and TRMM satellite measurements is given in Fig.  
73 9. The results of the statistical analysis are also shown in this figure. The comparison between the EANET surface  
74 observations and the WRF model simulations showed that the model generally reproduced the observed monthly  
75 precipitation adequately, with an R of 0.56, an NMB of +24.2%, and an NME of +64.7%. However, as shown in Figs. 2–8,  
76 the model tended to overestimate low precipitation levels (see Fig. 9 for the dry season). As has been discussed for Figs. 2–8,  
77 this overestimation may be the reason for the mismatch between the simulated and observed the wet deposition of S, N, and  
78 A. Resolving this problem is important for improving simulations of wet deposition. Meanwhile, in the comparison between  
79 the EANET surface observations and the satellite measurements, the statistical scores were superior to those obtained  
80 between the modeled and observed data, with an R of 0.77, an NMB of +5.9%, and an NME of +39.5%. The correspondence  
81 between EANET surface observations and satellite measurements was better (relative to the correspondence between the  
82 modeled and observed data) for monthly precipitation of less than 50 mm. From this result, it is expected that the adjustment  
83 based on satellite measurements has the potential to improve the original simulation of wet deposition. The spatial



84 distributions of precipitation from the WRF simulation and TRMM satellite measurements are respectively presented in  
85 Supplemental Figs. 1 and 2, and the adjustment factors for each month are given in Supplemental Fig. 3.

86

## 87 **4.2 Improvements of wet deposition modeling through a precipitation-adjusted approach for each country in** 88 **Southeast Asia**

### 89 **4.2.1 Myanmar**

90 At the Yangon (No. 30) site in Myanmar, the wet deposition of S, N, and A was underestimated, with an NMB exceeding –  
91 70%, as listed in Table 2. Table 2 also provides the results of the statistical analysis for the AO and AS approaches,  
92 demonstrating that the underestimation in the ENS was improved by both approaches; most of the statistical scores were  
93 improved compared with the ENS, though there was still underestimation compared with the observed wet deposition of S,  
94 N, and A. Fig. 10 shows the annual accumulated wet deposition of S, N, and A from the observational data, ENS, AO, and  
95 AS. As shown in the figure, the wet deposition was higher with the AO and AS approaches compared with ENS; that is, the  
96 underestimation was partly improved. Fig. 10 also shows the fractions of wet deposition occurring during the dry and wet  
97 seasons as bar graphs for the observational data, ENS, AO, and AS. It can be clearly seen that, for the wet deposition of S, N,  
98 and A, the fraction during the dry season was overestimated with ENS but was well matched with the AO and AS  
99 approaches.

00

### 01 **4.2.2 Thailand**

02 The wet depositions of S, N, and A was generally underestimated at the six sites in Thailand, as shown in Table 3. The  
03 statistical scores for AO and AS are also provided in this table. For the R value and the NME, AO and AS obtained superior  
04 values for Thailand compared with the ENS, showing a stronger correlation with the observational data. For AO and AS, the  
05 R values ranged from 0.61 to 0.85 for the wet depositions of S, N, and A, and the NMB was improved by 20–30% compared  
06 with the ENS. Fig. 11 shows the annual accumulated wet deposition of S, N, and A from observational data, ENS, AO, and  
07 AS, and the fractions of deposition occurring in the dry and wet seasons. From this figure, it can be seen that, compared with  
08 the ENS, the AO and AS approaches obtained superior values of the fractions of wet deposition during the dry and wet  
09 seasons at all six sites in Thailand. For Bangkok (No. 31), Samutprakarn (No. 32), and Pathumthani (No. 33), the  
10 underestimation in ENS was improved and the annual accumulated wet deposition of S, N, and A was close to the observed  
11 value for both AO and AS. Meanwhile, at Khanchanaburi (No. 34) and Chiang Mai (No. 36), the overestimation in ENS was  
12 improved and the annual accumulated wet deposition of S, N, and A was close to the observed value for both AO and AS.  
13 These results clarify that the precipitation-adjusted approach was effective to solve both overestimation and underestimation  
14 problems in the original simulated wet deposition. However, it should be noted that, for Nakhon Ratchasima (No. 35),



15 although the fractions of wet deposition occurring during the dry and wet seasons were improved with the AO and AS  
16 approaches, underestimation was worsened.

17

#### 18 **4.2.3 Cambodia**

19 At Phnom Penh (No. 38) in Cambodia, there were some difficulties capturing the wet deposition of S, N, and A using the  
20 ENS. As shown in Table 4, there was a low correlation between the observed values and the ENS for the wet deposition of S,  
21 and an even lower correlation for the wet deposition of N and A. The NMB was around  $-70\%$  and the NME was  $70\text{--}80\%$  for  
22 the wet deposition of S, N, and A using the ENS. These deficiencies in the ENS were adequately improved using AO and  
23 AS. For AO and AS, all statistical scores showed an improvement compared with the ENS. Fig. 12 shows the annual  
24 accumulated wet deposition of S, N, and A from observational data, ENS, AO, and AS, and the fraction of deposition  
25 occurring in the dry and wet seasons at Phnom Penh. It was also found that the ENS mismatched the fraction of wet  
26 deposition compared with the observed value, whereas AO and AS obtained more accurate fractions, as well as more  
27 accurate values of the annual accumulated wet deposition.

28

#### 29 **4.2.4 Vietnam**

30 For the four EANET sites in Vietnam, the statistical scores for the ENS were superior to those for other countries in  
31 continental Southeast Asia. In most cases, for AO and AS, the scores were improved compared with the ENS for the wet  
32 deposition of S, N, and A, as shown in Table 5. Fig. 13 shows the annual accumulated wet deposition of S, N, and A from  
33 observational data, ENS, AO, and AS, and the fraction of wet deposition occurring in the dry and wet seasons in Vietnam.  
34 Compared with other countries in continental Southeast Asia, the fraction of wet deposition occurring during the dry and wet  
35 seasons was better predicted by the ENS, and AO and AS performed similarly. However, for AS, the fraction during the wet  
36 season was overestimated at Hoa Binh (No. 41) and underestimated at Cuc Phuong (No. 42). Additionally, the overestimated  
37 wet deposition amount of S, N, and A at Da Nang (No. 39) led to a discrepancy with the observed results.

38

#### 39 **4.2.5 Philippines**

40 For the three EANET sites in the Philippines, it was found that the model overestimated the precipitation during the dry  
41 season. Fig. 14 presents the annual accumulated wet deposition of S, N, and A for the observational data, ENS, AO, and AS,  
42 and the fraction of the wet deposition occurring in the dry and wet seasons in Philippines. As shown in the figure, the ENS  
43 overestimated the fraction during the wet season at all sites for the wet depositions of S, N, and A. However, with AO and  
44 AS, this overestimation was improved and the simulated values were close to the observed ones. The statistical scores are  
45 listed in Table 6. As shown in the table, R was not changed or slightly increased and NME was improved, but NMB was not



46 improved. As shown in Fig. 14, this result was related to the change in model performance at Metro Manila (No. 43); the  
47 annual accumulated wet deposition amounts of S, N, and A were markedly decreased and very different from the observed  
48 data.

49

#### 50 **4.2.6 Malaysia**

51 At the four EANET sites in Malaysia, no distinction was found between the dry and wet seasons. Fig. 15 shows the annual  
52 accumulated wet deposition of S, N, and A from observation, ENS, AO, and AS, while Table 7 lists the statistical scores. AO  
53 and AS generally obtained improved results compared with the ENS. In particular, the strikingly large overestimation of the  
54 wet deposition of A in the ENS (NMB and NME greater than 200%) was improved with AO and AS.

55 At Petaling Jaya (No. 46) and Tanah Rata (No. 47), the observed annual accumulated wet deposition of A was around 2000 g  
56 N ha<sup>-1</sup>, whereas the ENS value was nearly 8000 g N ha<sup>-1</sup>. This large overestimation was reduced by AO and AS, which  
57 obtained values close to the observed value.

58

#### 59 **4.2.7 Indonesia**

60 In Indonesia, during the short dry season, wet deposition showed a steep decline; however, models did not show such a  
61 dramatic decrease. As shown in Table 8, the statistical scores for AO and AS were mostly superior to those of the ENS; the  
62 moderate correlation found for the wet depositions of S, N, and A in the ENS were improved by AO and AS. For the wet  
63 deposition of S, the NMB of +65.6% and NME of +100.2% in the ENS were improved by AO and AS. Fig. 16 shows the  
64 annual accumulated wet deposition of S, N, and A from observational data, ENS, AO, and AS, and the fraction of wet  
65 deposition occurring in the dry and wet seasons in Indonesia. The overestimation of the fraction during the wet season  
66 obtained by the ENS was improved by AO, but there was no change with AS. Although the annual accumulated wet  
67 depositions of S, N, and A for the ENS were generally close to the observed values, AS showed further overestimation at  
68 Serpong (No. 53) and there was almost no change at Jakarta (No. 51).

69

#### 70 **4.3 Revision of the distribution of wet deposition over Southeast Asia**

71 Based on the analysis and statistical results of the precipitation-adjusted approaches using surface observations and satellite  
72 measurements, it was found that these approaches improved the simulation of the wet deposition amount, as well as the  
73 fraction of wet deposition occurring during the dry and wet seasons. Although there were still difficulties in some cases, the  
74 precipitation adjustment was shown to be an effective way to improve the simulated wet deposition. One of the advantages  
75 of the adjustment using satellite measurements is that it provides the spatial distribution of adjustment factors; hence, it is  
76 possible to revise the wet deposition mapping over the modeling domain. In Fig. 17, the annual accumulated wet depositions



77 of S, N, and A are mapped. Both the ENS and AS simulated hot spots with high depositions of S, N, and A in regions such  
78 as northern Vietnam, the southern Malay Peninsula, and Sumatra Island and Java Island in Indonesia. However, there were  
79 clear differences between AS and ENS. These differences were similar for the wet depositions of S, N, and A. As shown in  
80 Fig. 17, for ENS, overestimation occurred in the central part of continental Southeast Asia, such as Eastern Myanmar,  
81 Thailand, the western edge of Sumatra Island, the south of Java Island, and Sulawesi Island in Indonesia, the Philippines;  
82 meanwhile, ENS produced underestimation over northern Vietnam, the east of Sumatra Island, and the northern edge of Java  
83 Island and Kalimantan Island in Indonesia.

84 Finally, Fig. 18 shows the original and revised wet deposition amounts in the eight countries participating in EANET. This  
85 figure summarizes the annual accumulated wet depositions of S, N, and A by the country-scale summed amount. As can be  
86 seen from the differences between ENS and AS shown in Figs. 17, the revisions by AS were similar for the wet depositions  
87 of S, N, and A. For AS, over Vietnam, Malaysia, and Indonesia, the country-level wet depositions were revised upward,  
88 whereas they were revised downward in the other five countries. The magnitudes of these revisions were up to  $\pm 40\%$ . This  
89 result indicates the importance of the precipitation amount for the reproducibility of wet depositions, and that the revision of  
90 wet deposition by a precipitation-adjusted approach was critically needed for the accurate estimation of wet deposition. The  
91 results of this study suggest that an approach which applies the precipitation obtained from satellite measurements could be  
92 used as one of the methodologies in the Measurement–Model Fusion for Global Total Atmospheric Deposition (MMF-  
93 GTAD) project under the Global Atmosphere Watch (GAW) program of the World Meteorological Organization (WMO)  
94 (WMO GAW, 2017, 2019). In this study, we were able to revise the wet deposition mapping over Southeast Asia to achieve  
95 better modeling reproducibility compared with EANET.

96

## 97 **5 Conclusion**

98 MICS-Asia Phase III has been conducted to understand the current modeling capabilities for the wet deposition and  
99 comprehend air pollution in Asia. This study presented a detailed analysis over Southeast Asia. The ensemble means of the  
100 modeled wet depositions of S, N, and A from seven models were evaluated by comparison with the wet deposition observed  
101 by EANET. Generally, the ensemble model can capture the observed wet deposition; however, the models failed to capture  
102 the wet deposition, even using the ensemble mean, obtaining low correlations and/or large biases and errors. Based on a  
103 detailed analysis of the observed precipitation at each EANET observation site, it was found that this failure to capture the  
104 wet deposition was related to the poor representation of the precipitation amount. In some cases, the model did not  
105 adequately simulate the precipitation pattern during the dry and wet seasons.

106 To overcome this modeling difficulty for precipitation, in this study, two precipitation-adjusted approaches were applied  
107 using EANET surface observations and TRMM satellite measurements, respectively. Both approaches have been shown to  
108 be effective for improving the modeling of the wet depositions of S, N, and A. To use satellite measurements of



09 precipitation, the spatial mappings of wet depositions were further revised. It was found that the original modeled wet  
10 deposition was overestimated over the central part of continental Southeast Asia, the western edge of Sumatra Island, the  
11 south of Java Island and Sulawesi Island in Indonesia, and the Philippines, and was underestimated over northern Vietnam,  
12 the east of Sumatra Island and the northern edge of Java Island and Kalimantan Island in Indonesia. For the country-scale  
13 accumulation of wet depositions, the wet deposition amounts were revised by up to  $\pm 40\%$  by the precipitation-adjusted  
14 approaches. Similar differences were found for wet depositions of S, N, and A; upward corrections were required for  
15 Vietnam, Malaysia, and Indonesia, whereas downward corrections were required for Myanmar, Thailand, Lao PDR,  
16 Cambodia, and the Philippines. The use of meteorological models could cause large errors related to precipitation patterns,  
17 as found in this study, and the use of meteorological model ensembles could be a possible way to obtain more accurate air  
18 quality model simulations (e.g., Kajino et al., 2019b). The precipitation-adjustment approach was effective at most sites;  
19 however, no improvement was found at other sites. The understanding of the mechanisms of the wet deposition process itself  
20 should be further investigated and inter-compared in the future Phase IV.

21

## 22 **Data availability**

23 The EANET wet deposition data used in this study are available at: <https://monitoring.eanet.asia/document/public/index>. The  
24 TRMM satellite precipitation measurements were downloaded from: <https://doi.org/10.5067/TRMM/TMPA/MONTH/7>. The  
25 model results of MICS-Asia Phase III are available upon request.

26

## 27 **Supplement**

28 The supplement related to this article is available online at: <https://doi.org/10.5194/acp-XX-XXXX-XXXX-supplement>.

29

## 30 **Author contributions**

31 SI led the deposition analysis group in MICS-Asia III, performed one of the model simulations, and prepared the manuscript  
32 with contributions from all co-authors. BG and KS are members of the deposition analysis group in MICS-Asia III and  
33 discussed the results with SI. ZW conducted the meteorological simulation driving the CTM simulation. JK prepared the  
34 emission inventory data for Southeast Asia and discussed the results from the viewpoint of emissions. TJ, JSF, XW, KY,  
35 TN, JL, BG, and MK performed the model simulations and contributed to submit their simulated deposition results. MICS-  
36 Asia III was coordinated by GRC and ZW.



37

## 38 **Competing interests**

39 The authors declare that they have no conflict of interest.

40

## 41 **Acknowledgements**

42 The authors thank EANET for providing the wet deposition observational data. The authors are grateful for the satellite  
43 measurement dataset from TRMM.

44

## 45 **References**

46 Akimoto, H., Nagashima, T., Li, J., Fu, J.S., Ji, D., Tan, J., and Wang, Z.: Comparison of surface ozone simulation among  
47 selected regional models in MICS-Asia III – effects of chemistry and vertical transport for the causes of difference,  
48 *Atmos. Chem. Phys.*, 19, 603–615, <https://doi.org/10.5194/acp-19-603-2019>, 2019.

49 Akimoto, H., Nagashima, T., Li, J., Fu, J.S., and Wang, Z.: Discrepancies between MICS-Asia III simulation and  
50 observation for surface ozone in the marine atmosphere over the Northwestern Pacific Asian rim region, *Atmos. Chem.*  
51 *Phys. Discuss.*, in review, <https://doi.org/10.5194/acp-2020-228>.

52 Appel, K. W., Foley, K. M., Bash, J. O., Pinder, R. W., Dennis, R. L., Allen, D. J., and Pickering, K.: A multi-resolution  
53 assessment of the community multiscale air quality (CMAQ) model v4.7 wet deposition estimates for 2002–2006,  
54 *Geosci. Model Dev.*, 4, 357–371, 2011.

55 Byun, D. and Schere, K. L.: Review of the governing equations, computational algorithms, and other components of the  
56 models-3 Community Multiscale Air Quality (CMAQ) modeling system, *Appl. Mech. Rev.*, 59, 51–77,  
57 <https://doi.org/10.1115/1.2128636>, 2006.

58 Carmichael, G. R., Calori, G., Hayami, H., Uno, I., Cho, S. Y., Engardt, M., Kim, S. -B., Ichikawa, Y., Ikeda, Y., Woo, J. -  
59 H., Ueda, H., and Amann, M.: The MICS-Asia study: model intercomparison of long-range transport and sulfur  
60 deposition in East Asia, *Atmos. Environ.*, 36, 175–199, 2002.

61 Carmichael, G. R., Sakurai, T., Streets, D., Hozumi, Y., Ueda, H., Park, S. U., Fung, C., Han, Z., Kajino, M., Engardt, M.,  
62 Bennet, C., Hayami, H., Sartelet, K., Holloway, T., Wang, Z., Kannari, A., Fu, J., Matsuda, K., Thongboonchoo, N.,  
63 and Amann, M.: MICS-Asia II: The model intercomparison study for Asia Phase II methodology and overview of  
64 findings, *Atmos. Environ.*, 42, 3468–3490, 2008a.



- 65 Carmichael, G. R., Sandu, A., Chai, T., Daescu, D. N., Constantinescu, E. M., and Tang, Y.: Predicting air quality:  
66 Improvements through advanced methods to integrate models and measurements, *J. Comp. Phys.*, 227(7), 3540–3571,  
67 <https://doi.org/10.1016/j.jcp.2007.02.024>, 2008b.
- 68 Chan, C.K. and Yao, X.: Air pollution in mega cities in China, *Atmos. Environ.*, 42, 1–42, 2008.
- 69 Chen, L., Gao, Y., Zhang, M., Fu, J. S., Zhu, J., Liao, H., Li, J., Huang, K., Ge, B., Lee, H.-J., Wang, X., Lam, Y.-F., Lin, C-  
70 Y., Itahashi, S., Nagashima, T., Kajino, M., Yamaji, K., Wang, Z., and Kurokawa, J.: MICS-Asia III: Multi-model  
71 comparison and evaluation of aerosol over East Asia, *Atmos. Chem. Phys.*, 19, 11911–11937,  
72 <https://doi.org/10.5194/acp-19-11911-2019>, 2019.
- 73 EANET: Quality assurance/quality control (QA/QC) program for wet deposition monitoring in East Asia, available at:  
74 <https://www.eanet.asia/wp-content/uploads/2019/04/qaqcwet.pdf>, 2000, last access: 1 October 2020.
- 75 EANET: Technical manual for wet deposition monitoring in East Asia, available at: [https://www.eanet.asia/wp-](https://www.eanet.asia/wp-content/uploads/2019/04/techwet.pdf)  
76 [content/uploads/2019/04/techwet.pdf](https://www.eanet.asia/wp-content/uploads/2019/04/techwet.pdf), 2010, last access: 1 October 2020.
- 77 EANET: available at <https://www.eanet.asia>, last access: 1 October 2020a.
- 78 EANET: Data Report, available at: <https://monitoring.eanet.asia/document/public/index>, last access: 1 October 2020b.
- 79 Gao, M., Han, Z., Liu, Z., Li, M., Xin, J., Tao, Z., Li, J., Kang, J. -E., Huang, K., Dong, X., Zhuang, B., Li, S., Ge, B., Wu,  
80 Q., Cheng, Y., Wang, Y., Lee, H. -J., Kim, C. -H., Fu, J. S., Wang, T., Chin, M., Woo, J. -H., Zhang, Q., Wang, Z., and  
81 Carmichael, G. R.: Air quality and climate change, Topic 3 of the Model Inter-Comparison Study for Asia Phase III  
82 (MICS-Asia III)–Part 1: Overview and model evaluation, *Atmos. Chem. Phys.*, 18, 4859–4884,  
83 <https://doi.org/10.5194/acp-18-4859-2018>, 2018.
- 84 Gao, M., Han, Z., Tao, Z., Li, J., Kang, J. -E., Huang, K., Dong, X., Zhuang, B., Li, S., Ge, B., Wu, Q., Lee, H. -J., Kim, C. -  
85 H., Fu, J. S., Wang, T., Chin, M., Li, M., Woo, J. -H., Cheng, Y., Wang, Z., and Carmichael, G. R.: Air quality and  
86 climate change, Topic 3 of the Model Inter-Comparison Study for Asia Phase III (MICS-Asia III)–Part 2: aerosol  
87 radiative effects and aerosol feedbacks, *Atmos. Chem. Phys.*, 20, 1147–1161, [https://doi.org/10.5194/acp-20-1147-](https://doi.org/10.5194/acp-20-1147-2020)  
88 2020, 2020.
- 89 Ge, B. Z., Wang, Z. F., Xu, X. B., Wu, J. B., Yu, X. L., and Li, J.: Wet deposition of acidifying substances in different  
90 regions of China and the rest of East Asia: Modeling with updated NAQPMS, *Environ. Pollut.*, 187, 10–21, 2014.
- 91 Ge, B., Itahashi, S., Sato, K., Xu, D., Wang, J., Fan, F., Tan, Q., Fu, J. S., Wang, X., Yamaji, K., Nagashima, T., Li, J.,  
92 Kajino, M., Liao, H., Zhang, M. G., Wang, Z., Li, M., Woo, J.-H., Kurokawa, J., Pan, Y., Wu, Q., Liu, X., and Wang, Z.  
93 F.: Model inter-comparison study for Asia (MICS-Asia) phase III: multimodel comparison of reactive nitrogen  
94 deposition over China, *Atmos. Chem. Phys.*, 20, 10587–10610, <https://doi.org/10.5194/acp-20-10587-2020>, 2020.
- 95 Hayami, H., Sakurai, T., Han, Z., Ueda, H., Carmichael, G. R., Streets, D., Holloway, T., Wang, Z., Thongboonchoo, N.,  
96 Engardt, M., Bennet, C., Fung, C., Chang, A., Park, S. U., Sartelet, K., Matsuda, K., and Amann, M.: MICS-Asia II:  
97 Model intercomparison and evaluation of particulate sulfate, nitrate and ammonium, *Atmos. Environ.*, 42, 3510–3527,  
98 2008.



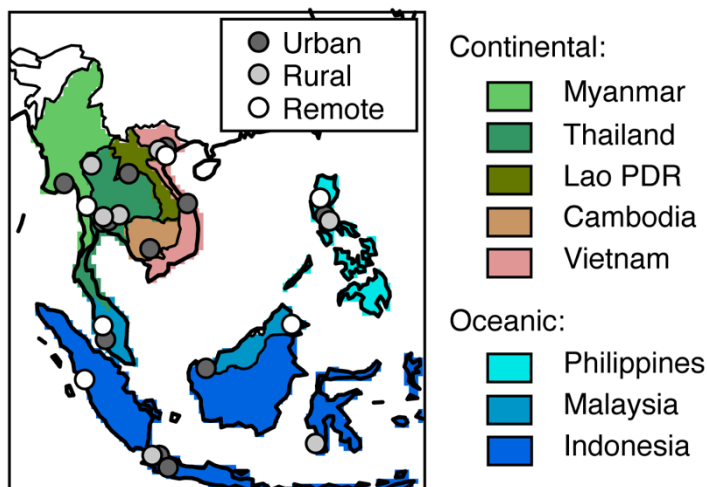
- 99 Huffman, G. J., Adler, R. F., Bolvin, D. T., Gu, G., Nelkin, E. J., Bowman, K. P., Stocker, E. F., and Wolff, D. B.: The  
00 TRMM multi-satellite precipitation analysis: Quasi-global, Multi-year, Combined-sensor precipitation estimates at fine  
01 scale. *J. Hydrometeor.*, 8, 38–55, 2007.
- 02 Itahashi, S.: Toward synchronous evaluation of source apportionments for atmospheric concentration and deposition of  
03 sulfate aerosol over East Asia, *J. Geophys. Res.*, 123, 2927–2953, 2018.
- 04 Itahashi, S., Ge, B. Z., Sato, K., Fu, J. S., Wang, X. M., Yamaji, K., Nagashima, T., Li, J., Kajino, M., Liao, H., Zhang, M.  
05 G., Wang, Z., Li, M., Kurokawa, J., Carmichael, G. R., and Wang, Z. F.: MICS-Asia III: overview of model  
06 intercomparison and evaluation of acid deposition over Asia, *Atmos. Chem. Phys.*, 20, 2667–2693,  
07 <https://doi.org/10.5194/acp-20-2667-2020>, 2020.
- 08 Itahashi S., Uno I., Irie H., Kurokawa J., and Ohara T.: Impacts of biomass burning emissions on tropospheric NO<sub>2</sub> vertical  
09 column density over continental Southeast Asia, in: *Land-Atmospheric Research Applications in South and Southeast*  
10 *Asia*, Springer Remote Sensing/Photogrammetry, edited by: Vadrevu K., Ohara T., Justice C., Springer, Cham, 67–81,  
11 [https://doi.org/10.1007/978-3-319-67474-2\\_4](https://doi.org/10.1007/978-3-319-67474-2_4), 2018.
- 12 Kajino, M., Deushi, M., Sekiyama, T. T., Oshima, N., Yumimoto, K., Tanaka, T. Y., Ching, J., Hashimoto, A., Yamamoto,  
13 T., Ikegami, M., Kamada, A., Miyashita, M., Inomata, Y., Shima, S., Takami, A., Shimizu, A., Hatakeyama, S.,  
14 Sadanaga, Y., Irie, H., Adachi, K., Zaizen, Y., Igarashi, Y., Ueda, H., Maki, T., and Mikami, M.: NHM-Chem, the  
15 Japan Meteorological Agency’s regional meteorology - chemistry model: model evaluations toward the consistent  
16 predictions of the chemical, physical and optical properties of aerosols, *J. Meteor. Soc. Jpn.*, 97(2), 337–374,  
17 <https://doi.org/10.2151/jmsj.2019-020>, 2019a.
- 18 Kajino, M., Sekiyama, T. T., Igarashi, Y., Katata, G., Sawada, M., Adachi, K., Zaizen, Y., Tsuruta, H., and Nakajima, T.:  
19 Deposition and dispersion of radio-caesium released due to the Fukushima nuclear accident: Sensitivity to  
20 meteorological models and physical modules, *J. Geophys. Res. Atmos.*, 124, 1823–1845.  
21 <https://doi.org/10.1029/2018JD028998>, 2019b.
- 22 Kong, L., Tang, X., Zhu, J., Wang, Z., Fu, J. S., Wang, X., Itahashi, S., Yamaji, K., Nagashima, T., Lee, H. -J., Kim, C. -H.,  
23 Lin, C. -Y., Chen, L., Zhang, M., Tao, Z., Li, J., Kajino, M., Liao, H., Sudo, K., Wang, Y., Pan, Y. -P., Tang, G., Li,  
24 M., Wu, Q., Ge, B., and Carmichael, G. R.: Evaluation and uncertainty investigation of the NO<sub>2</sub>, CO and NH<sub>3</sub> modeling  
25 over China under the framework of MICS-Asia III, *Atmos. Chem. Phys.*, 20, 181–202, [https://doi.org/10.5194/acp-20-](https://doi.org/10.5194/acp-20-181-2020)  
26 [181-2020](https://doi.org/10.5194/acp-20-181-2020), 2020.
- 27 Li, J., Nagashima, T., Kong, L., Ge, B., Yamaji, K., Fu, J. S., Wang, X., Fan, Q., Itahashi, S., Lee, H. -J., Kim, C. -H., Lin,  
28 C. -Y., Zhang, M., Tao, Z., Kajino, M., Liao, H., Li, M., Woo, J. -H., Kurokawa, J., Wu, Q., Akimoto, H., Carmichael,  
29 G. R., and Wang, Z.: Model evaluation and inter-comparison of surface-level ozone and relevant species in East Asia in  
30 the context of MICS-Asia phase III Part I: Overview, *Atmos. Chem. Phys.*, 19, 12993–13015,  
31 <https://doi.org/10.5194/acp-19-12993-2019>, 2019.



- 32 Li, J., Yang, W., Wang, Z., Chen, H., Hu, B., Li, J., Sun, Y., Fu, P., and Zhang, Y.: Modeling study of surface ozone source-  
33 receptor relationships in East Asia, *Atmos. Res.*, 167, 77–88, 2016.
- 34 Li, M., Zhang, Q., Kurokawa, J., Woo, J. -H., He, K. B., Lu, Z., Ohara, T., Song, Y., Streets, D. G., Carmichael, G. R.,  
35 Cheng, Y. F., Hong, C. P., Huo, H., Jiang, X. J., Kang, S. C., Liu, F., Su, H., and Zheng, B.: MIX: a mosaic Asian  
36 anthropogenic emission inventory for the MICS-Asia and the HTAP projects, *Atmos. Chem. Phys.*, 17, 935–963,  
37 <https://doi.org/10.5194/acp-17-935-2017>, 2017.
- 38 Liu, X. J., Zhang, Y., Han, W. X., Tang, A. H., Shen, J. L., Cui, Z. L., Vitousek, P., Erisman, J. W., Goulding, K., Christie,  
39 P., Fangmeier, A., and Zhang, F. S.: Enhanced nitrogen deposition over China, *Nature*, 494, 459–462, 2013.
- 40 Lin, N-H, Tsay, S. C., and Maring, H. B.: An overview of regional experiments on biomass burning aerosols and related  
41 pollutants in Southeast Asia: from BASE-ASIA and the Dongsha Experiment to 7-SEAS, *Atmos. Environ.*, 78:1–19,  
42 2013.
- 43 Reid, J. S., Hyer, E. J., Johnson R. S., et al.: Observing and understanding the Southeast Asian aerosol system by remote  
44 sensing: an initial review and analysis for the Seven Southeast Asian Studies (7SEAS) program, *Atmos. Res.*, 122:403–  
45 468, 2013.
- 46 Saya, A., Yoshikane, T., Chang, E.-C., Yoshimura, K., and Oki, T.: Precipitation redistribution method for regional  
47 simulations of radioactive material transport during the Fukushima Daiichi Nuclear Power Plant accident, *J. Geophys.*  
48 *Res. Atmos.*, 123, 10248–10259. <https://doi.org/10.1029/2018JD028531>, 2018.
- 49 Skamarock, W. C., Klemp, J. B., Dudhia, J., Gill, D. D., Barker, D. M., Duda, M. G., Huang, X. -Y., Wang, W., and Powers,  
50 J. G.: A description of the advanced research WRF version 3, *Nat. Cent. Atmos. Res.*, Boulder, CO, NCAR Technical  
51 Note, NCAR/TN-475+STR, 113 pp., 2008.
- 52 Solazzo, E., Bianconi, R., Pirovano, G., Matthias, V., Vautard, R., Appel, K. W., Bessagnet, B., Brandt, J., Christensen, J.  
53 H., Chemel, C., Coll, I., Ferreira, J., Forkel, R., Francis, X. V., Grell, G., Grossi, P., Hansen, A., Miranda, A. I., Moran,  
54 M. D., Nopmongco, U., Parnk, M., Sartelet, K. N., Schaap, M., D. Silver, J., Sokhi, R. S., Vira, J., Werhahn, J., Wolke,  
55 R., Yarwood, G., Zhang, J., Rao, S. T., and Galmarin, S.: Model evaluation and ensemble modelling of surface-level  
56 ozone in Europe and North America in the context of AQMEII, *Atmos. Environ.*, 53(6), 60–74, 2012.
- 57 Tan, J. N., Fu, J. S., Carmichael, G. R., Itahashi, S., Tao, Z. N., Huang, K., Dong, X. Y., Yamaji, K., Nagashima, T., Wang,  
58 X. M., Liu, Y. M., Lee, H. J., Lin, C. Y., Ge, B. Z., Kajino, M., Zhu, J., Zhang, M. G., Liao, H., and Wang, Z. F.: Why  
59 do models perform differently on particulate matter over East Asia? A multi-model intercomparison study for MICS-  
60 Asia III, *Atmos. Chem. Phys.*, 20, 7393–7410, <https://doi.org/10.5194/acp-20-7393-2020>, 2020.
- 61 Tropical Rainfall Measuring Mission (TRMM): TRMM (TMPA/3B43) Rainfall Estimate L3 1 month 0.25 degree × 0.25  
62 degree V7, Greenbelt, MD, Goddard Earth Sciences Data and Information Services Center (GES  
63 DISC), <https://doi.org/10.5067/TRMM/TMPA/MONTH/7>, 2011, last access: 28 October 2020.
- 64 Vadrevu K.P. and Justice C.O.: Vegetation fires in the Asian region: satellite observational needs and priorities, *Global*  
65 *Environ. Res.*, 15, 65–76, 2011.



- 66 Vet, R., Artz, R. S., Carou, S., Shaw, M., Ro, C. -U., Aas, W., Baker, A., Bowersox, V. C., Dentener, F., Galy-Lacaux, C.,  
67 Hou, A., Piennar, J. J., Gillett, R., Forti, M. C., Gromov, S., Hara, H., Khodzher, T., Mahowald, N. M., Nickovic, S.,  
68 Rao, P. S. P., and Reid, N. W.: A global assessment of precipitation chemistry and deposition of sulfur, nitrogen, sea  
69 salt, base cations, organic acids, acidity and pH, and phosphorous, *Atmos. Environ.*, 93, 3–100,  
70 <https://doi.org/10.1016/j.atmosenv.2013.10.060>, 2014.
- 71 Wang, Z., Xie, F., Sakurai, T., Ueda, H., Han, Z., Carmichael, G. R., Streets, D., Engards, M., Hollowway, T., Hayami, H.,  
72 Kajino, M., Thongboonchoo, N., Bennet, C., Park, S. U., Fung, C., Chang, A., Sartelet, K., and Amann, M.: MICS-Asia  
73 II: Model inter-comparison and evaluation of acid deposition, *Atmos. Environ.*, 42, 3528–3542,  
74 <https://doi.org/10.1016/j.atmosenv.2007.12.071>, 2008.
- 75 World Meteorological Organization Global Atmosphere Watch (WMO GAW): Global Atmosphere Watch Workshop on  
76 Measurement-Model Fusion for Global Total Atmospheric Deposition (MMF-GTAD), World Meteorological  
77 Organization, Geneva, Switzerland, GAW Report No. 234, 2017.
- 78 World Meteorological Organization Global Atmosphere Watch (WMO GAW): Global Atmosphere Watch Expert Meeting  
79 on Measurement-Model Fusion for Global Total Atmospheric Deposition, World Meteorological Organization, Geneva,  
80 Switzerland, GAW Report No. 250, 2019.
- 81 Zhang, Y., Mathur, R., Bash, J. O., Hogrefe, C., Xing, J., and Roselle, S.J.: Long-term trends in total inorganic nitrogen and  
82 sulfur deposition in the US from 1990 to 2010, *Atmos. Chem. Phys.*, 18, 9091–9106, [https://doi.org/10.5194/acp-18-](https://doi.org/10.5194/acp-18-9091-2018)  
83 [9091-2018](https://doi.org/10.5194/acp-18-9091-2018), 2018.
- 84



85

86

87

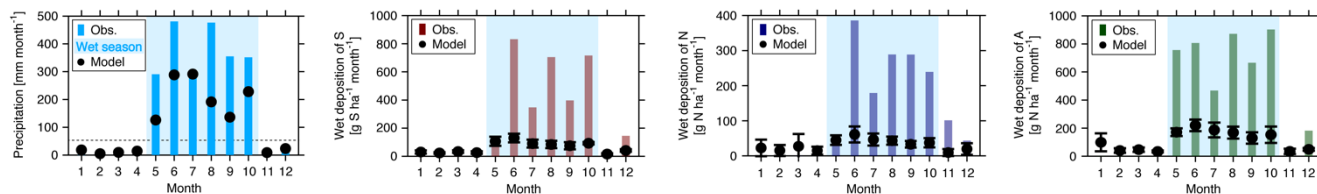
88

89

**Figure 1:** Map of Southeast Asia. Circles with different colors indicate observation sites classified as remote (white), rural (light gray), and urban (dark gray) by the Acid Deposition Monitoring Network in East Asia (EANET). Map colors indicate the eight countries participating in EANET in 2010. PDR, People's Democratic Republic.



30. Yangon



90

91

92

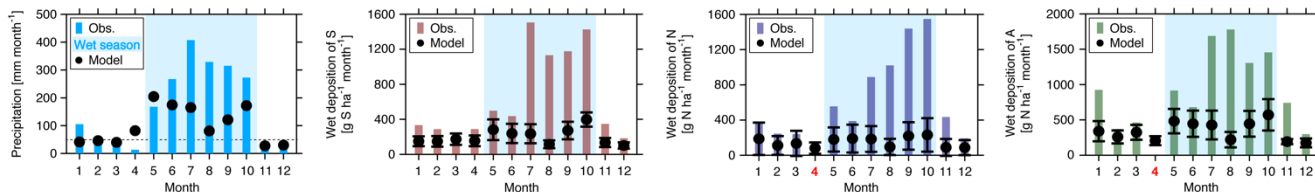
93

**Figure 2: Monthly accumulated precipitation and wet depositions of S, N, and A at Yangon, Myanmar. Whiskers represent the standard deviation among the seven models, and the wet season (light blue color) is defined as months when precipitation exceeded 50 mm.**

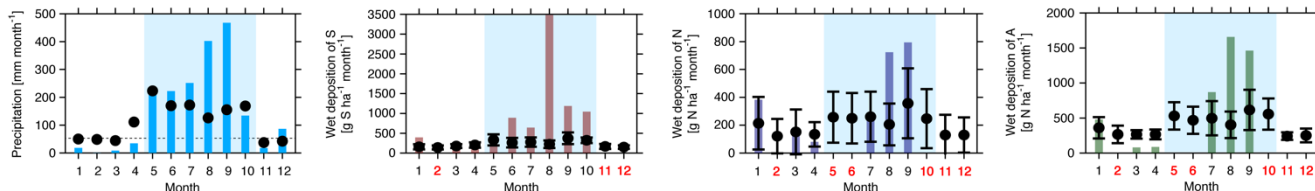
94



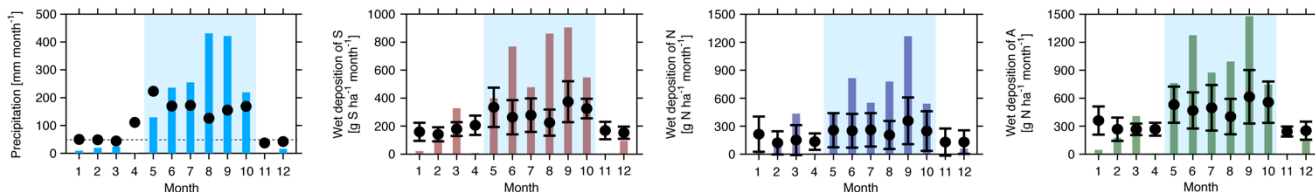
31. Bangkok



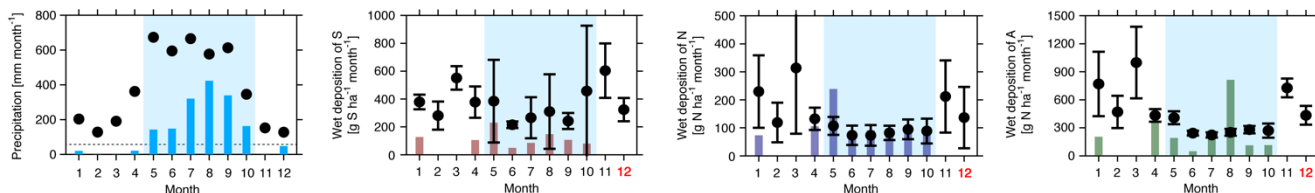
32. Samutprakarn



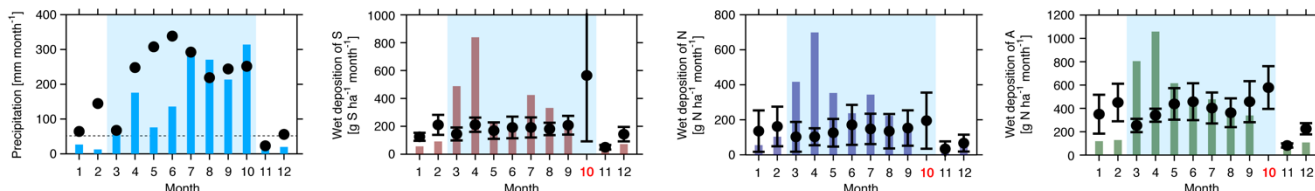
33. Pathumthani



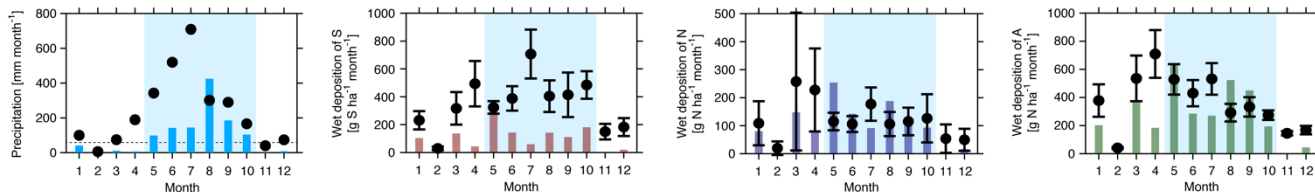
34. Khanchanaburi



35. Nakhon Ratchasima



36. Chiang Mai



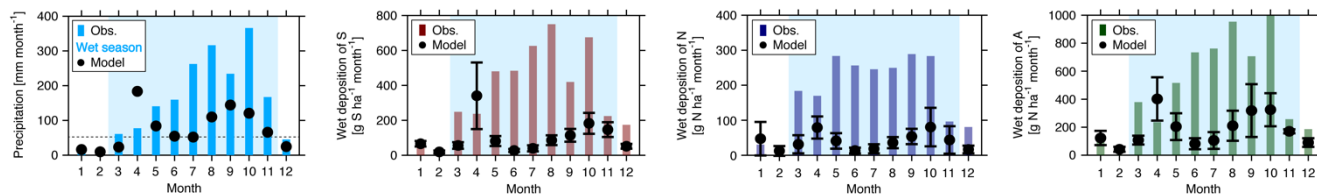
95

96 **Figure 3: Monthly accumulated precipitation and wet depositions of S, N, and A over Thailand. Whiskers represent the standard**  
 97 **deviation among the seven models, and the wet season (light blue color) is defined as months when precipitation exceeded 50 mm.**  
 98 **Months shown in red indicate a lack of observational data.**

99



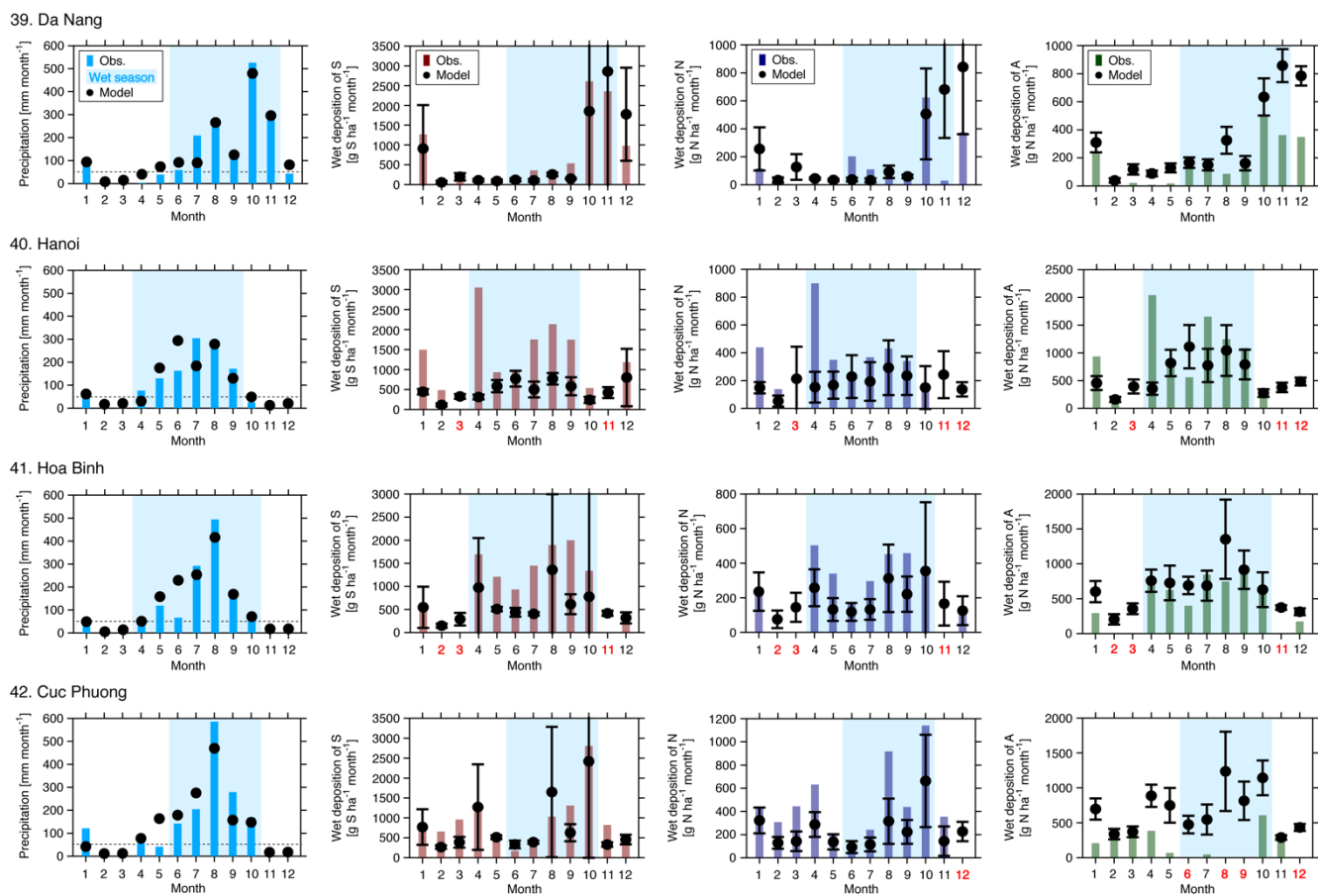
38. Phnom Penh



00

01 **Figure 4: Monthly accumulated precipitation and wet depositions of S, N, and A at Phnom Penh, Cambodia. Whiskers represent**  
02 **the standard deviation among the seven models, and the wet season (light blue color) is defined as months when precipitation**  
03 **exceeded 50 mm.**

04



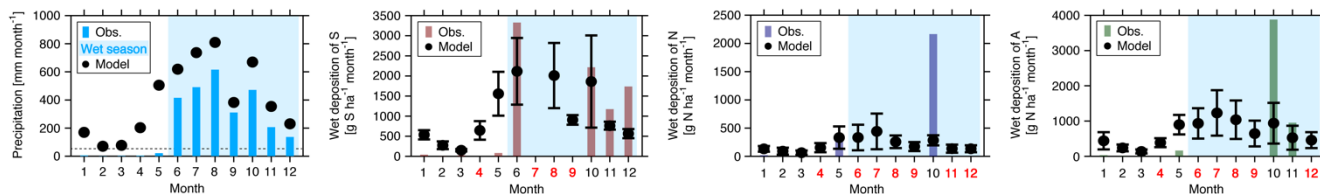
05

06 **Figure 5: Monthly accumulated precipitation and wet depositions of S, N, and A over Vietnam. Whiskers represent the standard**  
 07 **deviation among the seven models, and the wet season (light blue color) is defined as months when precipitation exceeded 50 mm.**  
 08 **Months shown in red indicate a lack of observational data.**

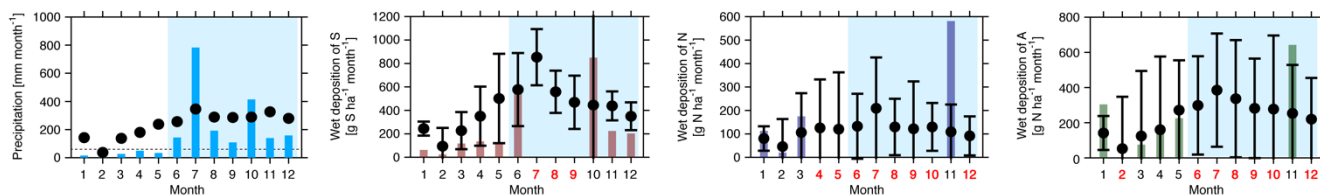
09



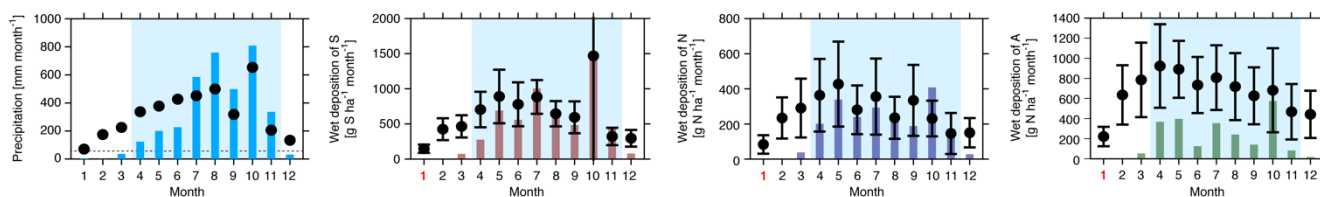
43. Metro Manila



44. Los Banos



45. Mt. Sto. Tomas

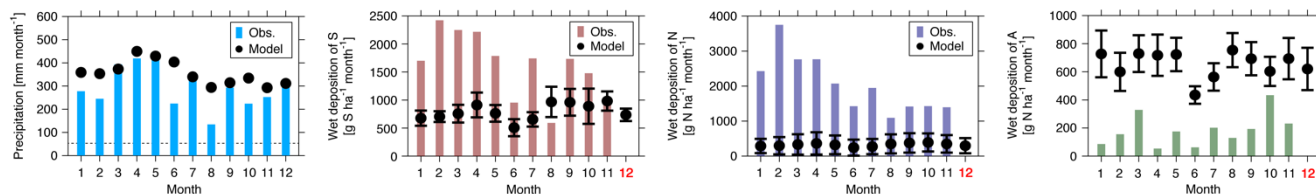


10  
 11  
 12  
 13  
 14

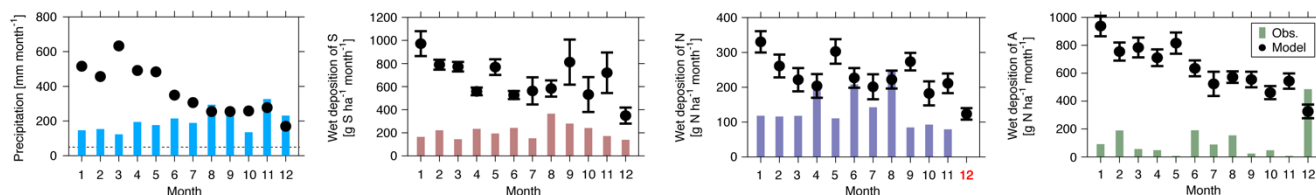
**Figure 6: Monthly accumulated precipitation and wet depositions of S, N, and A over the Philippines. Whiskers represent the standard deviation among the seven models, and the wet season (light blue color) is defined as months when precipitation exceeded 50 mm. Months shown in red indicate a lack of observational data.**



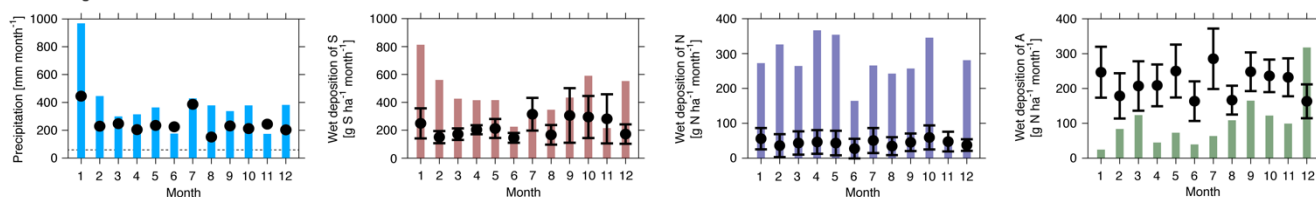
46. Petaling Jaya



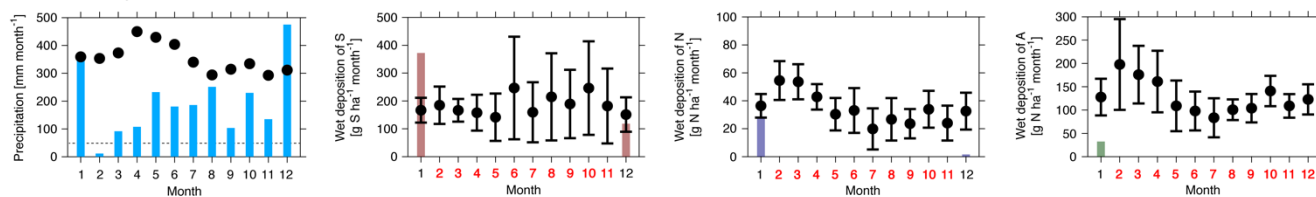
47. Tanah Rata



48. Kuching



49. Danum Valley



15

16

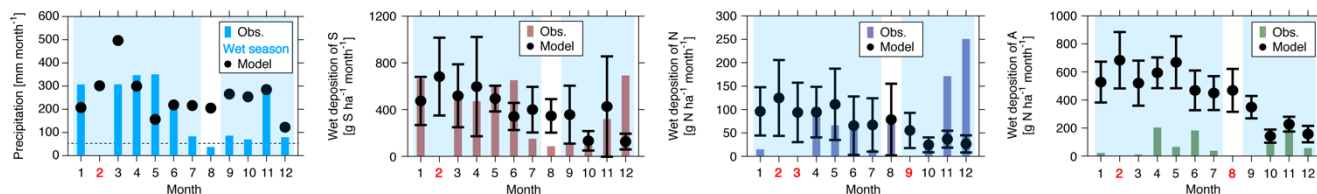
17

**Figure 7: Monthly accumulated precipitation and wet depositions of S, N, and A over Malaysia. Whiskers represent the standard deviation among the seven models. Months shown in red indicate a lack of observational data.**

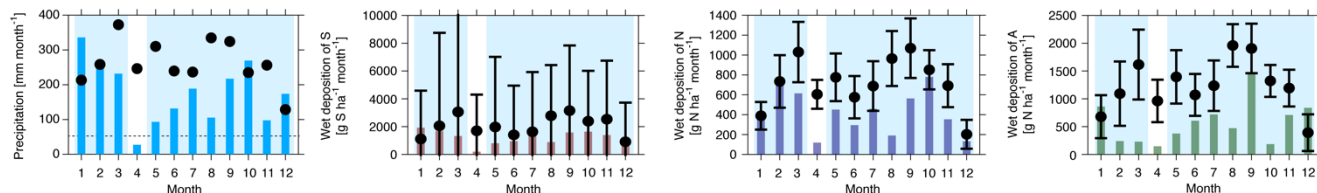
18



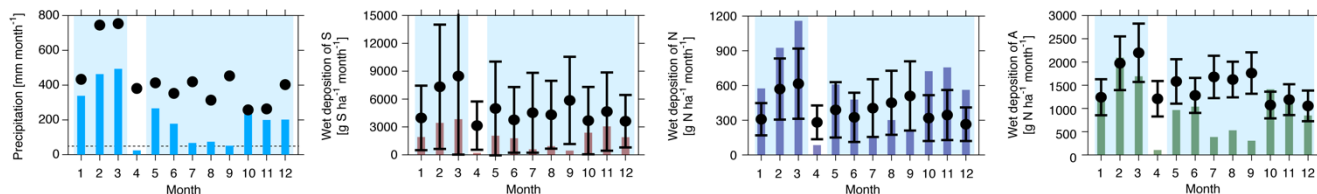
50. Kototabang



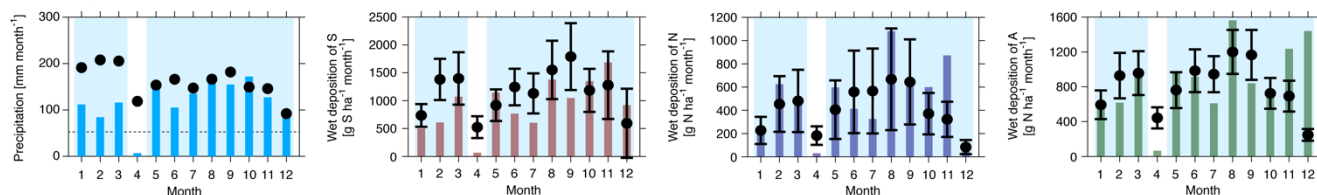
51. Jakarta



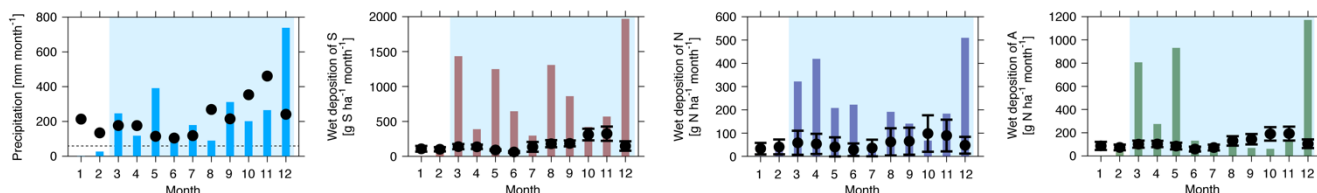
52. Bandung



53. Serpong

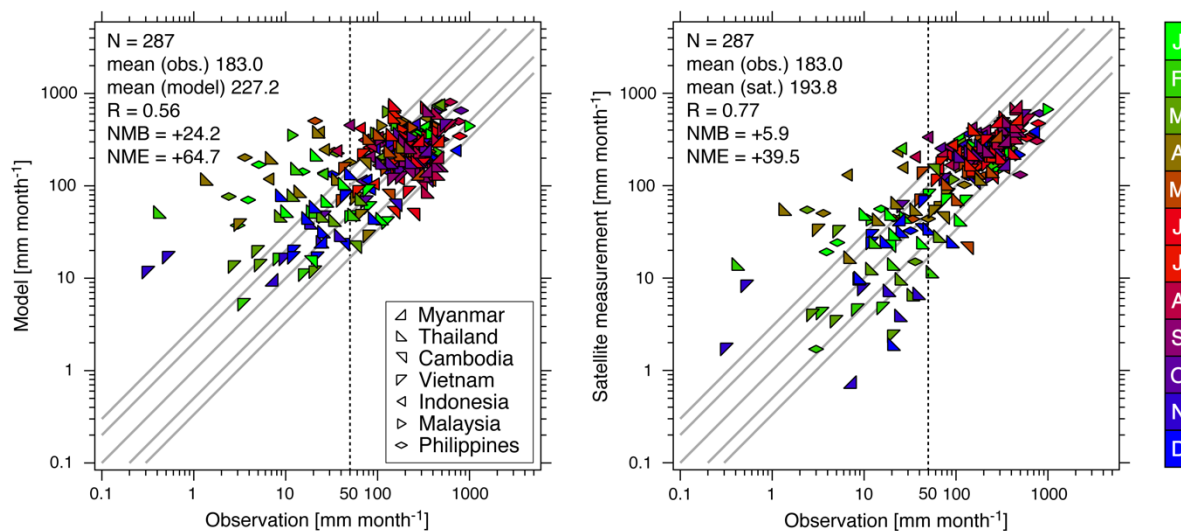


54. Maros



19

20 **Figure 8: Monthly accumulated precipitation and wet depositions of S, N, and A over Indonesia. Whiskers represent the standard**  
 21 **deviation among the seven models, and the wet season (light blue color) is defined as months when precipitation exceeded 50 mm.**  
 22 **Months shown in red indicate a lack of observational data.**  
 23

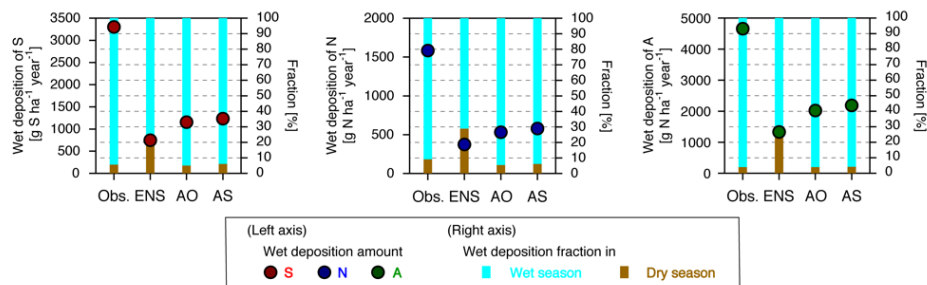


24  
25  
26  
27  
28  
29  
30

**Figure 9:** Scatter plots of the monthly precipitation amount over Southeast Asia comparing EANET surface observations with (left) model simulations and (right) satellite measurements. Symbols indicate different countries and colors indicate different months. In the inset, the statistical metrics of mean, correlation coefficient ( $R$ ), normalized mean bias (NMB), and normalized mean error (NME) are shown. The vertical dotted line represents observed precipitation of  $50 \text{ mm month}^{-1}$ , which defines the boundary between the dry and wet seasons in this study.



30. Yangon



31  
32  
33  
34  
35

**Figure 10: Observed and simulated annual accumulated wet deposition amounts of S, N, and A, and the fraction of wet deposition during the wet and dry seasons at Yangon, Myanmar. ENS, AO, and AS stand for the results of ensemble mean, precipitation adjustment by EANET observations, and precipitation adjustment by satellite observations, respectively.**

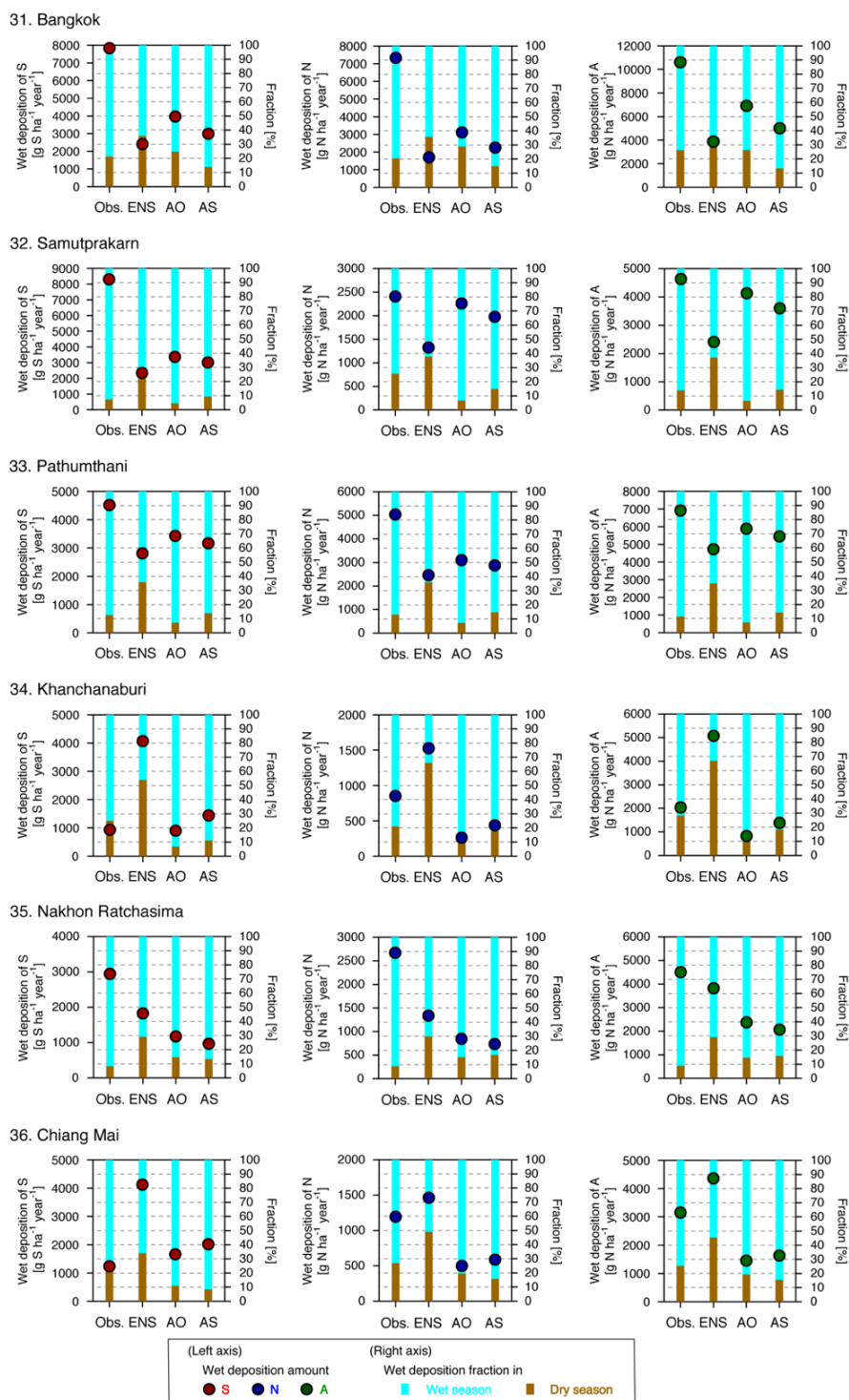
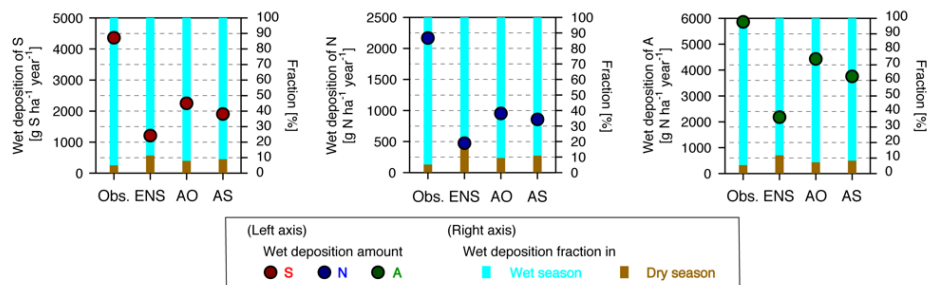


Figure 11: Observed and simulated annual accumulated wet deposition amounts of S, N, and A, and the fraction of wet deposition during the wet and dry seasons at six sites in Thailand. The annual accumulated wet deposition amount is based on the months in which wet deposition observations were available (see Fig. 3).

36  
 37  
 38  
 39  
 40

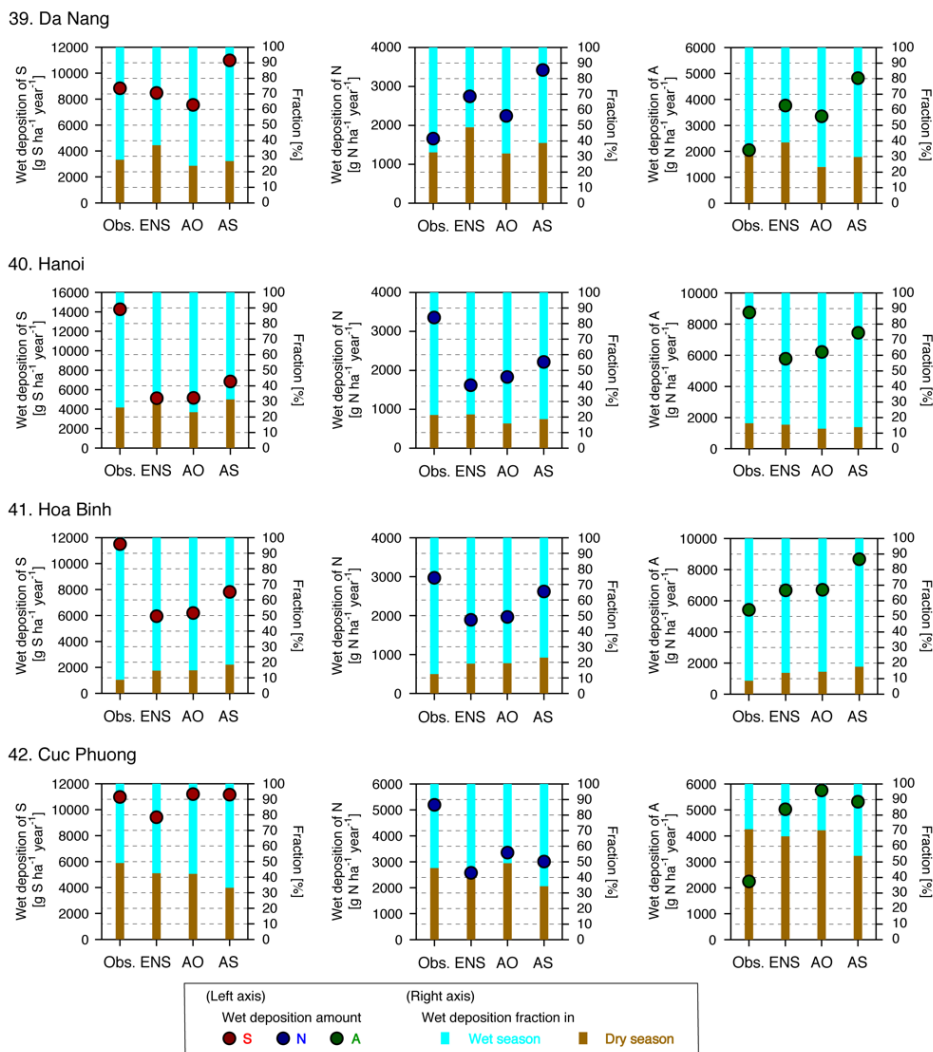


38. Phnom Penh



41  
 42  
 43  
 44

Figure 12: Observed and simulated annual accumulated wet deposition amounts of S, N, and A, and the fraction of wet deposition during the wet and dry seasons at Phnom Penh, Cambodia.



45  
 46  
 47  
 48  
 49

Figure 13: Observed and simulated annual accumulated wet deposition amounts of S, N, and A, and the fraction of wet deposition during the wet and dry seasons at four sites over Vietnam. The annual accumulated wet deposition amount is based on the months for which wet deposition observations were available (see Fig. 5).

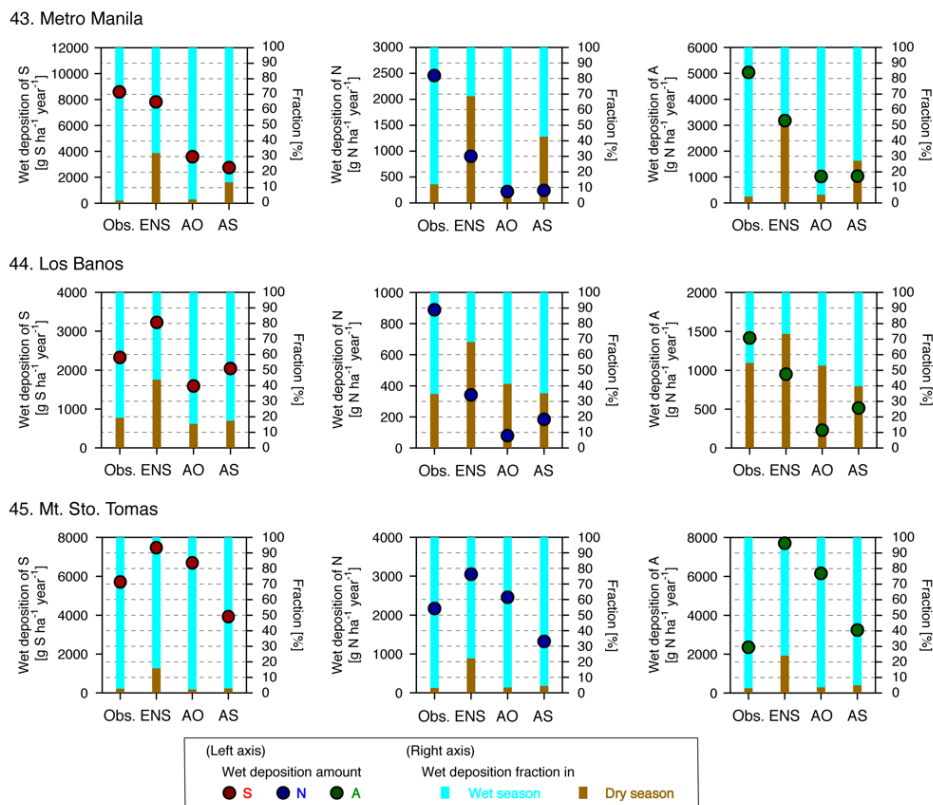
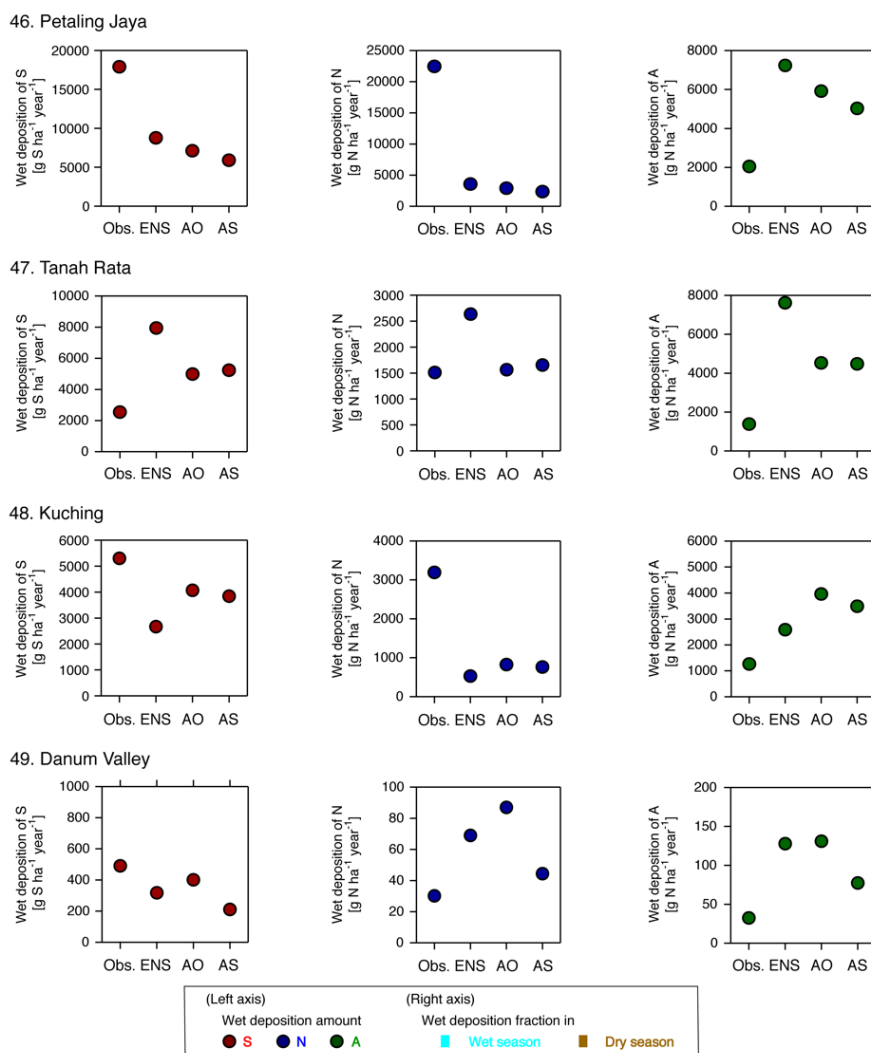


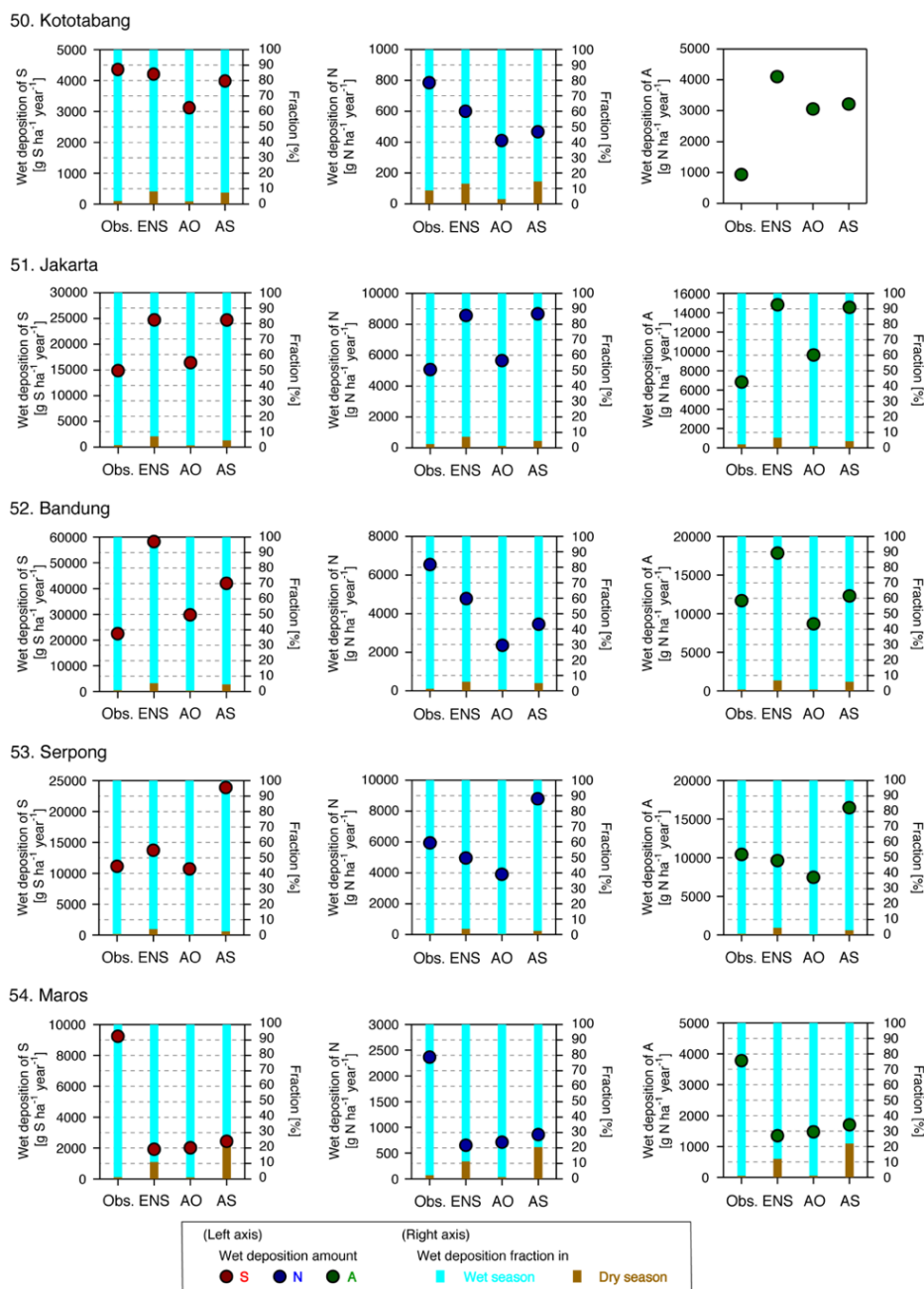
Figure 14: Observed and simulated annual accumulated wet deposition amounts of S, N, and A, and the fraction of wet deposition during the wet and dry seasons at three sites in the Philippines. The annual accumulated wet deposition amount is based on the months for which wet deposition observations were available (see Fig. 6).

50  
 51  
 52  
 53  
 54



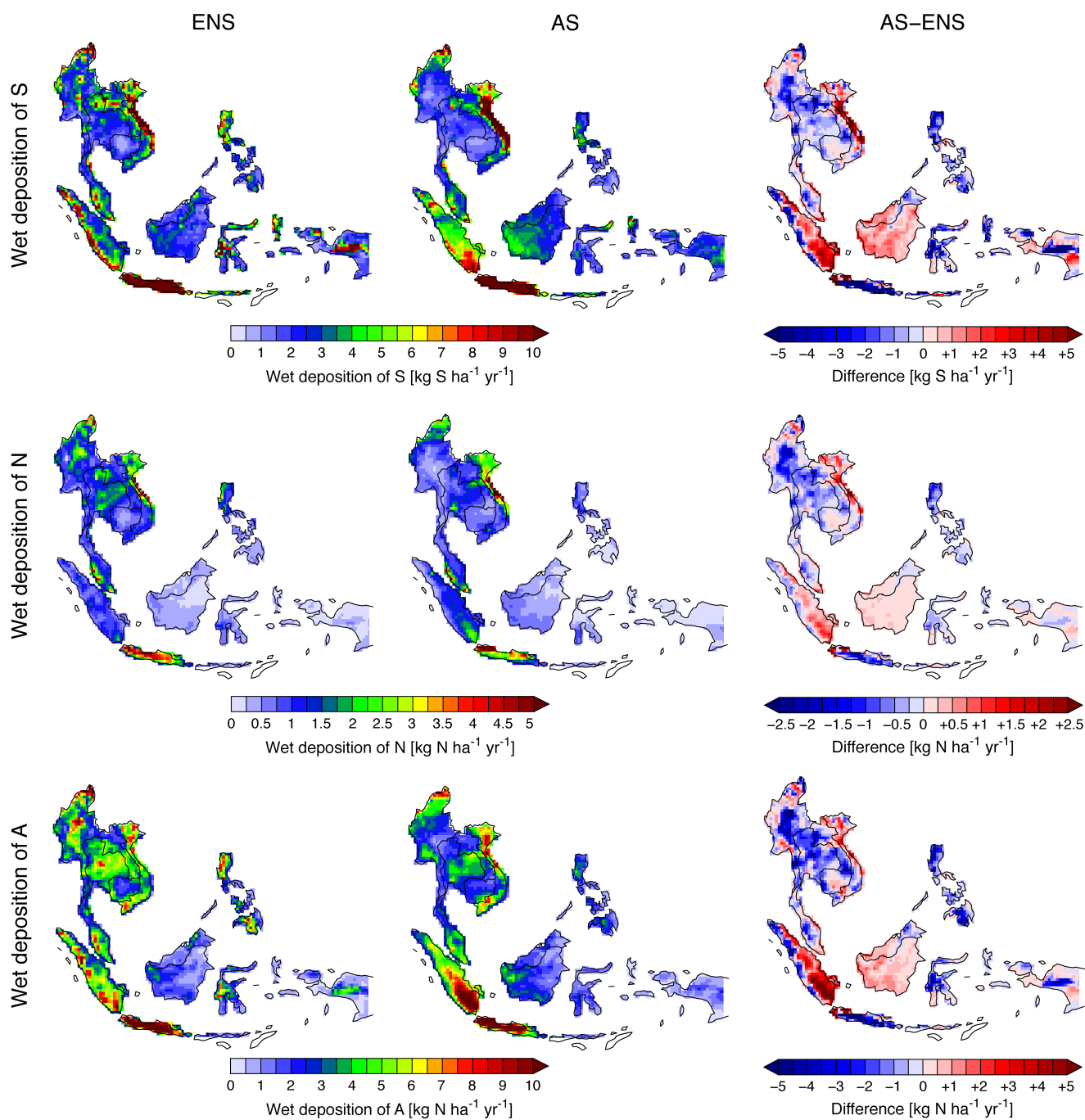
55  
 56  
 57  
 58  
 59

Figure 15: Observed and simulated annual accumulated wet deposition amounts of S, N, and A at four sites in Malaysia. The annual accumulated wet deposition amount is based on the months for which wet deposition observations were available (see Fig. 7).



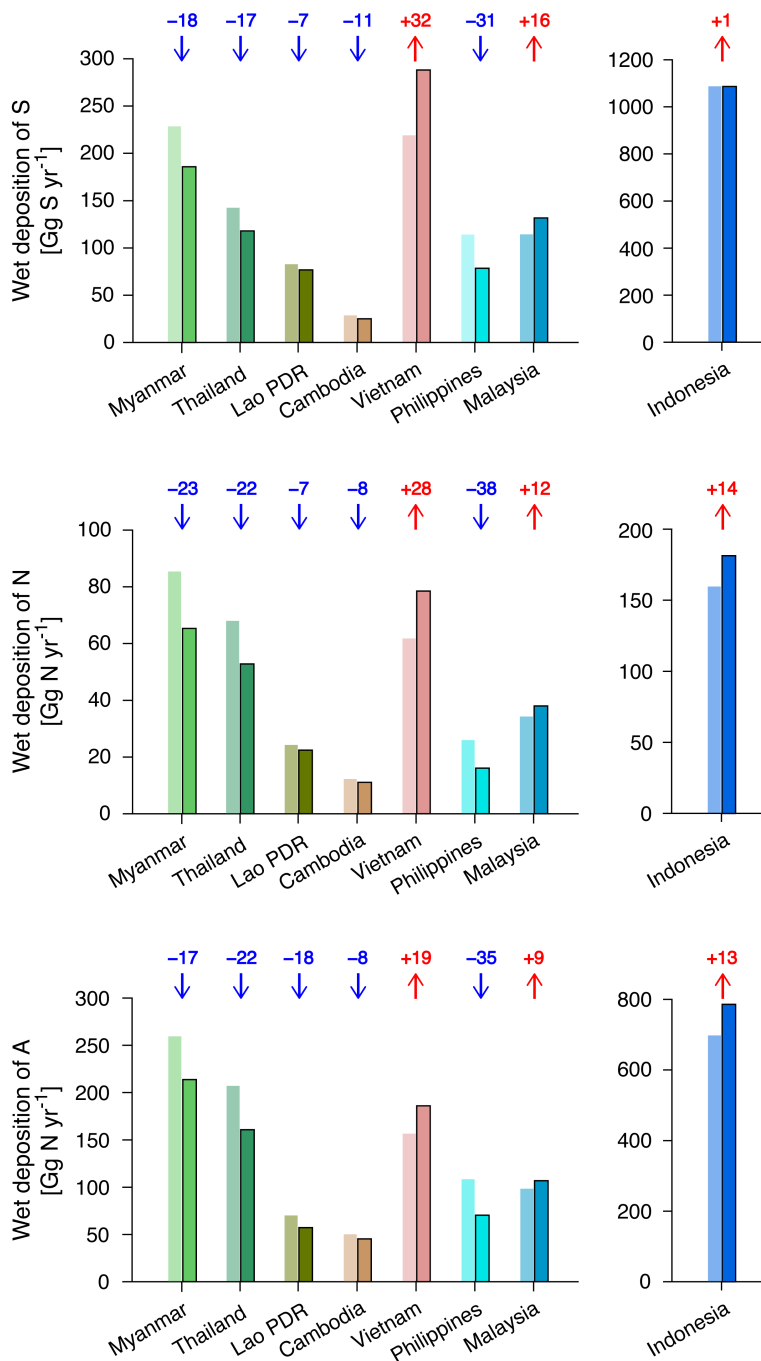
60  
 61  
 62  
 63  
 64

**Figure 16: Observed and simulated annual accumulated wet deposition amounts of S, N, and A, and the fraction of wet deposition during the wet and dry seasons at five sites in Indonesia. The annual accumulated wet deposition amount is based on the months for which wet deposition observations were available (see Fig. 8).**



65  
66 **Figure 17: Maps of the annual accumulated wet deposition of (top) S, (center) N, and (bottom) A calculated by (left) ENS, (middle)**  
67 **AS, and (right) the difference between AS and ENS. Note that the color scale is different for the wet deposition of N. Some**  
68 **locations around the Suva Sea (south of Flores Island, Sumba Island, and Timor Island) and the east of New Guinea Island shown**  
69 **in white are outside of the modeling domain.**

70



.71

.72 **Figure 18: Simulated annual accumulated wet deposition amounts of (top) S, (center) N, and (bottom) A over Southeast Asian**  
 .73 **countries calculated by ENS (light bars without outlines) and AS (dark bars outlined in black). Blue numbers with down-facing**  
 .74 **arrows indicate downward revision by AS and red numbers with upward-facing arrows indicate upward revision by AS.**

.75



76  
 77

**Table 1: Information of 25 Acid Deposition Monitoring Network in East Asia (EANET) observation sites located in Southeast Asia.**

Site no.	Country	Name	Latitude (°)	Longitude (°E)	Altitude (m a.s.l.)	Classification
30	Myanmar	Yangon	16.50	96.12	22	Urban
31	Thailand	Bangkok	13.77	100.53	2	Urban
32		Samutprakarn	13.73	100.57	2	Urban
33		Pathumthani	14.03	100.77	2	Rural
34		Khanchanaburi	14.77	98.58	170	Remote
35		Nakhon Ratchasima	14.45	101.88	418	Rural
36		Chiang Mai	18.77	98.93	350	Rural
37	Lao PDR	Vientiane	17.00	102.00	177	Urban
38	Cambodia	Phnom Penh	11.55	104.83	10	Urban
39	Vietnam	Da Nang	16.04	108.21	60	Urban
40		Hanoi	21.02	105.85	5	Urban
41		Hoa Binh	20.82	105.33	23	Rural
42		Cuc Phuong	20.25	105.72	155	Remote
43	Philippines	Metro Manila	14.63	121.07	54	Urban
44		Los Baños	14.18	121.25	35	Rural
45		Mt. Sto. Tomas	16.42	120.60	1500	Rural
46	Malaysia	Petaling Jaya	3.10	101.65	87	Urban
47		Tanah Rata	4.47	101.38	1470	Remote
48		Kuching	1.48	110.47	22	Urban
49		Danum Valley	4.98	117.85	427	Remote
50	Indonesia	Kototabang	-0.20	100.32	864	Remote
51		Jakarta	-6.18	106.83	7	Urban
52		Bandung	-6.90	107.58	743	Urban
53		Serpong	-6.25	106.57	46	Rural
54		Maros	-4.92	119.57	11	Rural

78 Note: Site nos. are unified with the overview paper of Itahashi et al. (2020). PDR, People's Democratic Republic.

79



80 **Table 2: Statistical analysis of the model performance for Yangon, Myanmar.**

	Wet deposition of S			Wet deposition of N			Wet deposition of A		
	ENS	AO	AS	ENS	AO	AS	ENS	AO	AS
N		12			12			12	
mean (observation)		275.0			132.0			388.1	
mean (model)	62.2	96.2	102.8	31.2	44.3	48.2	111.1	168.7	182.2
R	0.81	0.77	0.65	0.74	0.79	0.69	0.87	0.95	0.83
NMB [%]	-77.4	-65.0	-62.6	-76.4	-66.4	-63.5	-71.4	-56.4	-53.1
NME [%]	+84.2	+72.7	+72.0	+86.4	+72.2	+70.8	+82.1	+57.6	+53.2
FAC2 [%]	8.3	33.3	8.3	8.3	41.7	33.3	0.0	50.0	41.7
FAC3 [%]	16.7	50.0	50.0	16.7	58.3	41.7	8.3	75.0	66.7
FAC5 [%]	33.3	91.7	58.3	25.0	91.7	58.3	33.3	91.7	66.7

81 Note: Units are g S ha<sup>-1</sup> month<sup>-1</sup> for the wet deposition of S, and g N ha<sup>-1</sup> month<sup>-1</sup> for the wet depositions of N and A. Improvements in  
 82 the statistical score with AO and AS compared to ENS are highlighted in gray. ENS, ensemble mean; AO, adjusted by observation at  
 83 EANET sites; AS, adjusted by satellite measurements.  
 84



85 **Table 3: Statistical analysis of the model performance for six sites in Thailand.**

	Wet deposition of S			Wet deposition of N			Wet deposition of A		
	ENS	AO	AS	ENS	AO	AS	ENS	AO	AS
N		67			63			63	
mean (observation)		384.8			309.4			505.8	
mean (model)	262.4	216.3	202.9	155.8	160.0	140.7	385.4	342.5	304.5
R	-0.01	0.71	0.61	0.47	0.77	0.77	0.21	0.85	0.78
NMB [%]	-31.8	-43.8	-47.3	-49.6	-48.3	-54.5	-23.8	-32.3	-40.0
NME [%]	+86.9	+53.6	+64.3	+71.3	+53.6	+59.7	+70.8	+40.1	+48.3
FAC2 [%]	31.3	52.2	35.8	39.7	44.4	41.3	46.0	63.5	49.2
FAC3 [%]	59.7	77.6	62.7	63.5	66.7	55.6	65.1	82.5	65.1
FAC5 [%]	77.6	92.5	79.1	81.0	84.1	71.4	85.7	95.2	76.2

86 Note: Units are  $\text{g S ha}^{-1} \text{ month}^{-1}$  for the wet deposition of S, and  $\text{g N ha}^{-1} \text{ month}^{-1}$  for the wet depositions of N and A. Improvements in the  
 87 statistical score with AO and AS compared with ENS are highlighted in gray.  
 88



89 **Table 4: Statistical analysis of the model performance for Phnom Penh, Cambodia.**

	Wet deposition of S			Wet deposition of N			Wet deposition of A		
	ENS	AO	AS	ENS	AO	AS	ENS	AO	AS
N		12			12			12	
mean (observation)		363.7			180.7			488.6	
mean (model)	101.1	187.5	158.8	39.4	79.4	71.4	181.7	369.3	313.0
R	0.05	0.56	0.31	0.28	0.51	0.30	0.34	0.84	0.61
NMB [%]	-72.2	-48.4	-56.3	-78.2	-56.0	-60.5	-62.8	-24.4	-35.9
NME [%]	+78.8	+57.0	+66.2	+80.9	+60.1	+66.8	+69.9	+31.0	+50.8
FAC2 [%]	25.0	58.3	33.3	8.3	33.3	33.3	25.0	91.7	58.3
FAC3 [%]	25.0	66.7	66.7	25.0	66.7	41.7	50.0	91.7	91.7
FAC5 [%]	58.3	91.7	83.3	41.7	83.3	75.0	75.0	100.0	91.7

90 Note: Units are  $\text{g S ha}^{-1} \text{ month}^{-1}$  for the wet deposition of S, and  $\text{g N ha}^{-1} \text{ month}^{-1}$  for the wet depositions of N and A. Improvements in the  
 91 statistical score with AO and AS compared with ENS are highlighted in gray.

92



93 **Table 5: Statistical analysis of the model performance for four sites in Vietnam.**

	Wet deposition of S			Wet deposition of N			Wet deposition of A		
	ENS	AO	AS	ENS	AO	AS	ENS	AO	AS
N		43			41			55	
mean (observation)		1060.5			321.5			486.0	
mean (model)	673.5	700.3	756.1	215.4	249.0	274.9	559.1	579.6	590.9
R	0.63	0.67	0.67	0.47	0.59	0.48	0.46	0.57	0.60
NMB [%]	-36.5	-34.0	-19.3	-33.0	-23.9	-14.5	+15.0	+19.2	+22.2
NME [%]	+48.2	+46.6	+42.6	+55.8	+47.6	+54.7	+57.1	+52.6	+56.2
FAC2 [%]	53.5	51.2	60.5	48.8	56.1	65.9	41.8	41.8	41.8
FAC3 [%]	72.1	76.7	81.4	80.5	78.0	75.6	52.7	61.8	60.5
FAC5 [%]	93.0	95.3	83.7	87.8	85.4	82.9	56.4	65.5	56.4

94 Note: Units are  $\text{g S ha}^{-1} \text{ month}^{-1}$  for the wet deposition of S, and  $\text{g N ha}^{-1} \text{ month}^{-1}$  for the wet depositions of N and A. Improvements in the  
 95 statistical score with AO and AS compared with ENS are highlighted in gray.  
 96



97 **Table 6: Statistical analysis of the model performance for three sites in the Philippines.**

	Wet deposition of S			Wet deposition of N			Wet deposition of A		
	ENS	AO	AS	ENS	AO	AS	ENS	AO	AS
N		28			20			22	
mean (observation)		594.0			275.8			400.4	
mean (model)	661.5	216.3	202.9	214.6	137.9	87.4	538.2	336.7	217.7
R	0.79	0.78	0.74	0.25	0.23	0.39	0.35	0.26	0.45
NMB [%]	+11.4	-28.6	-46.7	-22.2	-50.0	-68.3	+34.4	-15.9	-45.6
NME [%]	+58.0	+45.1	+55.3	+75.1	+74.8	+70.2	+123.6	+102.9	+74.4
FAC2 [%]	53.6	71.4	60.7	55.0	45.0	40.0	22.7	13.6	40.9
FAC3 [%]	60.7	89.3	75.0	60.0	50.0	60.0	50.0	27.3	54.5
FAC5 [%]	78.6	96.4	82.1	65.0	55.0	70.0	59.1	59.1	72.7

98 Note: Units are  $\text{g S ha}^{-1} \text{ month}^{-1}$  for the wet deposition of S, and  $\text{g N ha}^{-1} \text{ month}^{-1}$  for the wet depositions of N and A. Improvements in the  
 99 statistical score with AO and AS compared with ENS are highlighted in gray.  
 00



01 **Table 7: Statistical analysis of model performance for four sites in Malaysia.**

	Wet deposition of S			Wet deposition of N			Wet deposition of A		
	ENS	AO	AS	ENS	AO	AS	ENS	AO	AS
N		37			36			36	
mean (observation)		709.2			755.8			131.5	
mean (model)	532.6	444.9	410.3	189.3	149.7	134.2	488.1	404.0	363.3
R	0.43	0.60	0.38	0.59	0.69	0.48	0.08	0.27	0.29
NMB [%]	-24.9	-36.8	-42.1	-74.9	-80.2	-82.2	+271.2	+207.2	+176.3
NME [%]	+69.7	+53.6	+54.1	+83.7	+83.4	+79.6	+284.5	+210.7	+180.6
FAC2 [%]	32.4	62.2	45.9	22.2	25.0	30.6	19.4	13.9	27.8
FAC3 [%]	73.0	83.8	70.3	33.3	36.1	33.3	33.3	41.7	41.7
FAC5 [%]	94.6	100.0	91.9	50.0	61.1	61.1	63.9	72.2	80.6

02 Note: Units are  $\text{g S ha}^{-1} \text{ month}^{-1}$  for the wet deposition of S, and  $\text{g N ha}^{-1} \text{ month}^{-1}$  for the wet depositions of N and A. Improvements in the  
 03 statistical score with AO and AS compared with ENS are highlighted in gray.  
 04



05 **Table 8: Statistical analysis of model performance for five sites in Indonesia.**

	Wet deposition of S			Wet deposition of N			Wet deposition of A		
	ENS	AO	AS	ENS	AO	AS	ENS	AO	AS
N		59			57			58	
mean (observation)		1052.5			363.2			580.5	
mean (model)	1743.1	1052.4	1644.9	343.3	228.9	390.4	823.8	466.9	856.3
R	0.68	0.89	0.71	0.56	0.70	0.57	0.47	0.45	0.50
NMB [%]	+65.6	0.0	+56.3	-5.5	-37.0	+7.5	+41.9	-2.3	+27.5
NME [%]	+100.2	+37.7	+86.1	+56.3	+49.2	+63.3	+79.3	+61.6	+43.9
FAC2 [%]	52.5	76.3	42.4	59.6	49.1	54.4	43.1	41.4	44.8
FAC3 [%]	71.2	83.1	69.5	73.7	71.9	73.7	50.0	53.4	58.6
FAC5 [%]	79.7	91.5	83.1	80.7	87.7	89.5	58.6	60.3	70.7

06 Note: Units are  $\text{g S ha}^{-1} \text{ month}^{-1}$  for the wet deposition of S, and  $\text{g N ha}^{-1} \text{ month}^{-1}$  for the wet depositions of N and A. Improvements in  
 07 the statistical score with AO and AS compared with ENS are highlighted in gray.